On the Ages of Resonant, Eroded and Fossil Asteroid Families

Andrea Milani[a], Zoran Knežević[b], Federica Spoto[d], Alberto Cellino[e], Bojan Novaković[f], Georgios Tsirvoulis[c]

[a] *Dipartimento di Matematica, Università di Pisa, Largo Pontecorvo 5,56127 Pisa, Italy*
[b] *Serbiam Academy of Sciences and Arts, Knez Mihajlova 35, 11000 Belgrade, Serbia*
[c] *Astronomical Observatory, Volgina 7, 11060 Belgrade 38, Serbia*
[d] *Laboratoire Lagrange, Universitè Côte d'Azur, Observatoire de la Côte d'Azur, CNRS*
[e] *INAF–Osservatorio Astrofisico di Torino, 10025 Pino Torinese, Italy*
[f] *Department of Astronomy, Faculty of Mathematics, University of Belgrade, Studentski trg 16, 11000 Belgrade, Serbia*

Abstract

In this work we have estimated 10 collisional ages of 9 families for which for different reasons our previous attempts failed. In general, these are difficult cases that required dedicated effort, such as a new family classifications for asteroids in mean motion resonances, in particular the 1/1 and 2/1 with Jupiter, as well as a revision of the classification inside the 3/2 resonance.

Of the families locked in mean motion resonances, by employing a numerical calibration to estimate the Yarkovsky effect in proper eccentricity, we succeeded in determining ages of the families of (1911) Schubart and of the "super-Hilda" family, assuming this is actually a severely eroded original family of (153) Hilda. In the Trojan region we found families with almost no Yarkovsky evolution, for which we could compute only physically implausible ages. Hence, we interpreted their modest dispersions of proper eccentricities and inclinations as implying that the Trojan asteroid families are fossil families, frozen at their proper elements determined by the original ejection velocity field. We have found a new family, among the Griquas locked in the 2/1 resonance with Jupiter, the family of (11097) 1994 UD1.

We have estimated the ages of 6 families affected by secular resonances: families of (5) Astraea, (25) Phocaea, (283) Emma, (363) Padua, (686) Ger-

Email address: milani@dm.unipi.it (Andrea Milani)

suind, and (945) Barcelona. By using in all these cases a numerical calibration method, we have shown that the secular resonances do not affect significanly the secular change of proper a.

For the family of (145) Adeona we could estimate the age only after removal of a number of assumed interlopers.

With the present paper we have concluded the series dedicated to the determination of asteroid ages with a uniform method. We computed the age(s) for a total of 57 families with > 100 members. For the future work there remain families too small at present to provide reliable estimates, as well as some complex families (221, 135, 298) which may have more ages than we could currently estimate. Future improvement of some already determined family ages is also possible by increasing family membership, revising the calibrations, and using more reliable physical data.

Keywords: Asteroids, dynamics; Impact Processes; Resonances, orbital; Trojan asteroids.

1. Introduction

In our previous work (Milani et al. (2014), hereinafter referred to as Paper I, and Knežević et al. (2014), Paper II), we have introduced new methods to classify asteroids into families, applicable to an extremely large dataset of proper elements, to update continuously this classification, and to estimate the collisional ages of large families. In later work (Spoto et al. (2015), Paper III, and in Milani et al. (2016), Paper IV), we have systematically applied a uniform method (an improvement of that proposed in Paper I) to estimate asteroid family collisional ages, and solved a number of problems of collisional models, including cases of complex relationship between dynamical families (identified by clustering in the proper elements space) and collisional families (formed at a single time of collision).

In this paper we solve several difficult cases of families for which either a collisional model had not been obtained, e.g., because it was not clear how many separate collisions were needed to form a given dynamical family, or because our method based on V-shapes (in the plane with coordinates proper semimajor axis a and inverse of diameter $1/D$) did not appear to work properly. In many cases the difficulty had to do with complex dynamics, such as the effects of resonances (either in mean motion or secular). In other cases the problem was due to the presence of interlopers (members of the family by the automatic classification but not originated from the same parent body) which can be identified by using physical data, including albedo, color indexes and absolute magnitudes.

Thus, to assess the level of success of the research presented in this paper, the reader should take into account that all the families discussed in this paper have been selected by the failure of our previous attempts to find a reasonable collisional model and/or to estimate an age. In this paper we discuss new family classifications for asteroids in mean motion resonances, in particular the 1/1 and 2/1 with Jupiter, plus a revision and critical discussion of the classification inside the 3/2 resonance. Overall we have estimated 10 additional ages for 9 families. Almost all the succesful computations have required some additional effort, on top of using the methods developed in our previous papers. Two examples: first, removal of interlopers has played a critical role in several cases, to the point that 2 of the 9 families used for age estimation have seen removal of the namesake asteroid as an inter-

loper, resulting in change of the family name[1]; second, the interaction of the Yarkovsky effect with resonances has very different outcomes: outside resonances, the semimajor axis undergoes a secular drift, while inside a mean motion resonance the semimajor axis is locked and other elements can undergo a secular drift. Inside a secular resonance the drift in semimajor axis appears not to be significantly affected, as shown by our numerical tests.

The paper is organized as follows: in Section 2 we deal with the specific problems of families formed by asteroids locked inside the strongest mean motion resonances with Jupiter, namely 3/2 (Hildas), 1/1 (Trojans), and 2/1 (Griquas). In Section 3 we discuss the families affected by secular resonances (involving the perihelia and nodes of the asteroid and the planets Jupiter and/or Saturn). In Section 4 we present two successful interpretations of families with strange shapes and many interlopers. In Section 5 we discuss the families for which we either have not found a consistent collisional model, or we have found a model (and computed an age) but there are still problems requiring dedicated observational efforts. In Section 6 we draw some conclusion, not just from this paper but from the entire series, in particular discussing the limitations to the possibility of further investigating the collisional history of the asteroid belt with the current data set.

The numerical data in connection with the computation of ages presented in this paper are collected in the Tables 1–8, analogous to those used in Papers III and IV: all the tables are given in the Appendix. Tables 1 and 2 describe the fit region in the $(e, 1/D)$ and $(a, 1/D)$ planes, respectively, where D is the diameter in km. Table 3 contains the albedo data from various sources, used to estimate D. Tables 4 and 5 contain the results of the fit for slopes of the V-shapes, again in the two planes. Table 6 contains the data to compute the Yarkovsky calibration (see Papers I and III), and finally Tables 7 and 8 contain the calibrations, the estimated ages and their uncertainties. Tables 2, 3, 5, 6 and 8 are partitioned by horizontal lines into sections for families of type fragmentation, of type cratering, and with one side only. We have found no additional young ages (< 100 My).

For the sake of brevity, unless absolutely necessary, we do not specifically quote in the text these tables and data they contain, but the reader is encour-

[1]We are using the traditional asteroid family naming convention, by which the family is named after the lowest numbered member: if the lowest numbered is an interloper, the second lowest numbered becomes the namesake.

aged to consult them whenever either some intermediate result is needed, or some quantitative support of the proposed explanation is required.

2. Families in mean motion resonances with Jupiter

Mean motion resonances with Jupiter give rise to the Kirkwood gaps, where the asteroid main belt has essentially empty regions corresponding to the most chaotic orbits: the main gaps correspond to the resonances 3/1 and 5/2. For the order 1 resonances 3/2 and 2/1 there are gaps created in the regions of strongly chaotic orbits but also islands of relative stability, where families can be found. The 1/1 resonance contains a large stable region containing the two Trojan swarms (preceding and following Jupiter).

2.1. 3/2 resonance: the Hilda region

The 3/2 mean motion resonance with Jupiter contains a large region in which the critical argument $2\lambda - 3\lambda_J + \varpi$ can librate for a very long time. The computation of proper elements specifically for the 3/2 resonant orbits is possible (Schubart, 1991), but not really necessary for the purpose of family classification. The reason is that most information is contained in the proper elements $(e, \sin I)$ (see Figure 1), while the value of the smoothed and averaged a is sharply constrained close to the libration center (see Figure 2). Thus we are using in this region "semi-proper" elements $(a, e, \sin I)$ computed with the same algorithm used for the non-resonant case, and some families can be identified by the HCM method all the same.

Two clusters are visible by eye in Figure 1, at low proper $\sin I$ the very well defined family of (1911) Schubart and at higher proper $\sin I$ a clan, that is a number of small families which may be interpreted as the remains of an eroded, very ancient family, which could have included the largest asteroid in the region, (153) Hilda.

The Schubart family

The most prominent family we have found in the Hilda region with our methods (Paper I, II) is the family of (1911) Schubart now grown to 508 members (of which 136 multiopposition, added in Paper IV).[2] The methods of Paper III to compute the age are not strictly applicable to this case, because the range in a is very narrow, only 0.035 au. Indeed a V-shape in

[2]This family had already been reported in Schubart (1991).

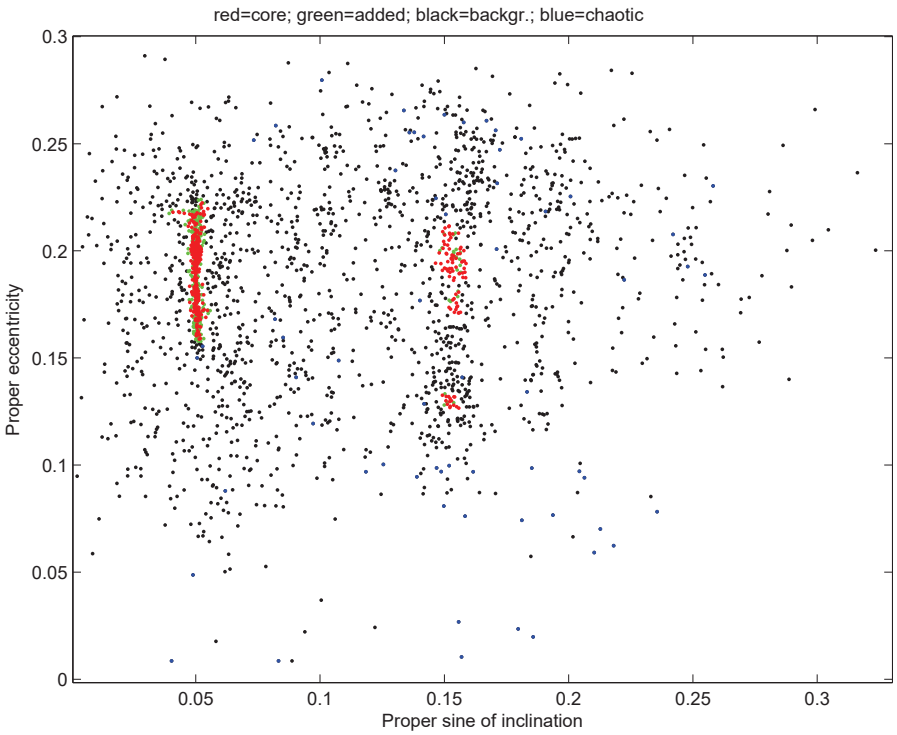

Figure 1: The Hilda region projected on the proper $(\sin I, e)$ plane. The visible concentrations are the family of (1911) Schubart on the left (around proper $\sin I = 0.05$) and the eroded family of (153) Hilda near the center (around proper $\sin I = 0.15$). The different number density indicates a different collisional and Yarkovsky history. Red points mark family members obtained by the standard HCM procedure, while green are members attributed in later updates (Papers I and II), the blue are chaotic.

the plane with coordinates proper a and $1/D$ is well defined but does not describe the amount of change in the proper elements due to the Yarkovsky effect: it is constrained by the slope of the libration curve in the region where the family is.

The Hildas remain locked in the 3/2 resonance (see Figure 2), thus the Yarkovsky effect pushes the eccentricity either up (for direct spin) or down (for retrograde spin) (Bottke et al., 2002). This results in a V-shape in the plane of proper e and $1/D$ (Figure 4), which can be used to estimate the age, provided the Yarkovsky calibration for de/dt is available.

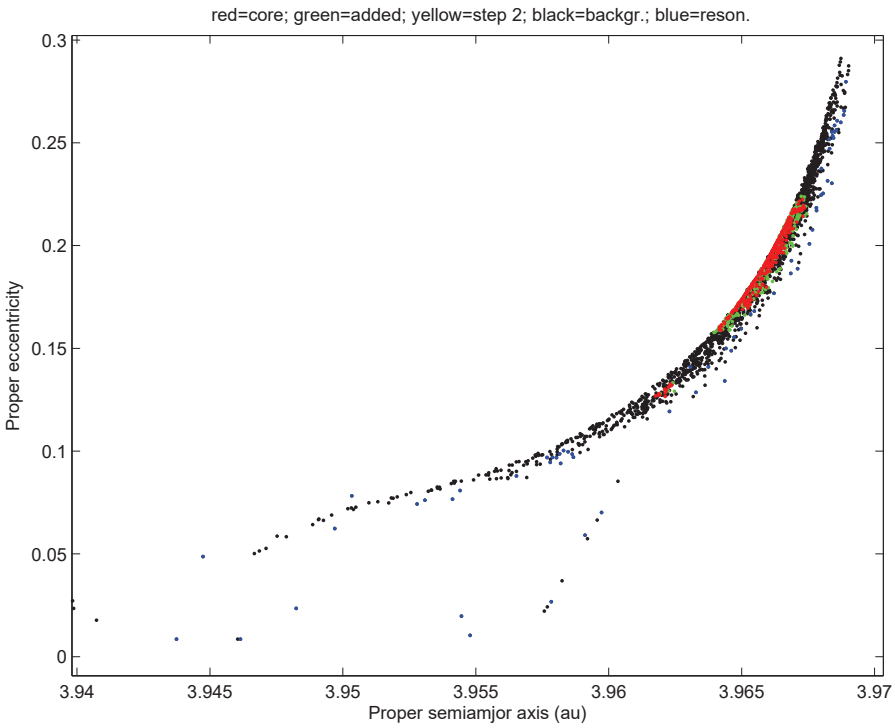

Figure 2: The Hilda region projected on the proper (a, e) plane. The averaging used to compute synthetic proper elements produces a narrow strip around the libration center line, the Yarkovsky driven secular changes can take place only along this line. Due to the blown-up scale in proper semimajor axis the libration center line appears strongly curved, but in reality the effect is small.

To obtain the calibration in de/dt we have used numerical experiments with a sample of 200 clones of the orbit of (1911) with values of non-resonant $da/dt(NR)$ assigned in the range $-3.6 \times 10^{-9} < da/dt(NR) < 3.6 \times 10^{-9}$ au/y. The integrations were performed for a time span of 10 My, then proper elements were computed for windows of 2 My, shifting by 1 My, giving a total of 9 data points for each clone. To these we fitted a de/dt obtaining the results shown in Figure 3. Then a regression line was fitted in the $(da/dt(NR), de/dt)$ plane:

$$\frac{de}{dt} = 0.335 \cdot \frac{da}{dt}(NR) \; ;$$

and the coefficient 0.335 has to be used to convert the da/dt calibration,

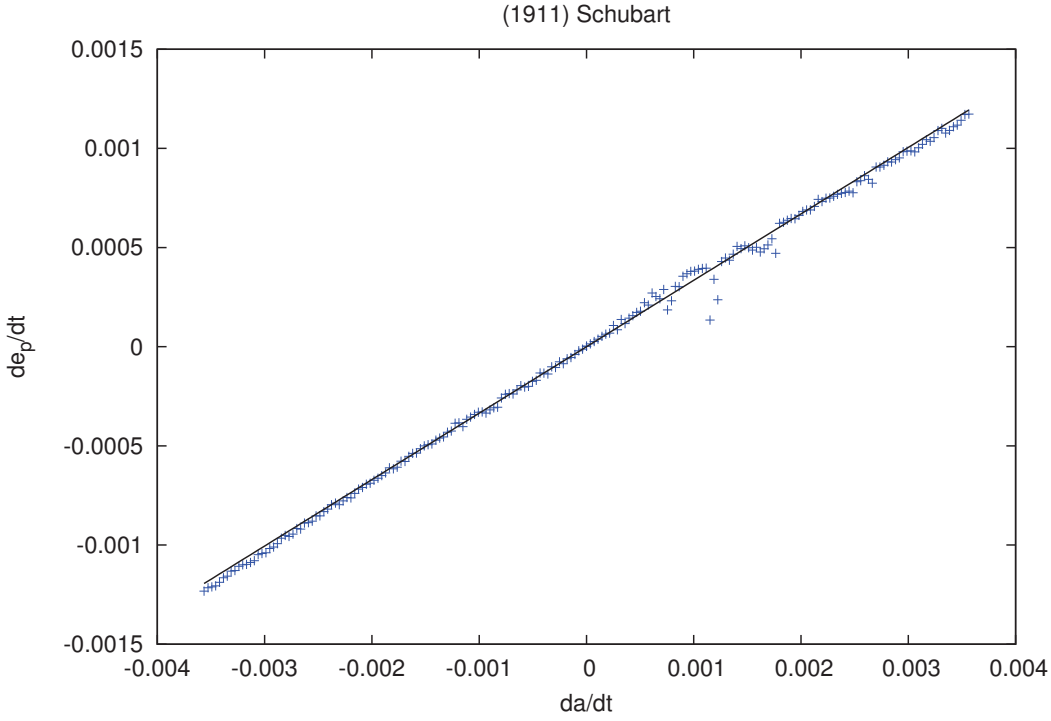

Figure 3: The eccentricity calibration of the Yarkovsky effect inside the 3/2 resonance, for the family of (1911) Schubart. On the horizontal axis, the value of da/dt (in au/My) as it would have been outside of the resonance; on the vertical axis the value of de/dt actually measured for a resonant orbit. The straight line is the regression line fitted to the 200 data points.

which we obtained with the same procedure used in Paper I and III, into a de/dt calibration.

The V-shape fit in $(e, 1/D)$ plane (Figure 4) reveals consistent slopes (see Table 4) and we can model this family as a single collisional family.

The Yarkovsky calibration converted in e is -1.68×10^{-10} in 1/y for the IN side and 1.72×10^{-10} for the OUT side, hence the age estimate is $1,547\pm492$ for IN, $1,566\pm484$ for OUT side, in My. Note that the uncertainty is completely dominated by the relative calibration uncertainty of 0.3, thus more work on calibration is needed.

The slight curvature of the libration center line of Figure 2 results in a slow motion also in proper a, but the secular da/dt is 0.016 times what it would

be outside the resonance. Thus, in principle, the age could be computed by using the V-shape in $(a, 1/D)$ and the calibration above, with similar results but poorer accuracy with respect to the results in the $(e, 1/D)$ plane.

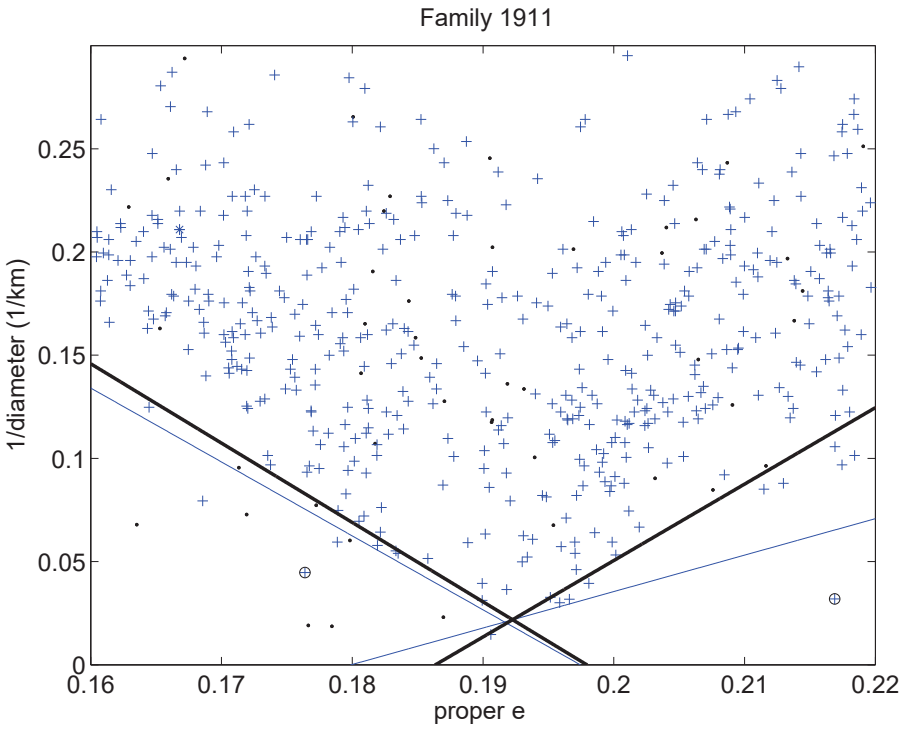

Figure 4: The V-shape for the family of (1911) Schubart in the plane $(e, 1/D)$, with the fit lines (blue the first iteration, black the final one). The crosses are family members, the one with also a circle are outliers discarded from the V-shape fit; dots are non-members.

The Hilda core and other small families

The high $\sin I$ portion of the 3/2 resonance shows some density contrast, see Figure 1: the rectangle with $0.075 < e < 0.29$ and $0.14 < \sin I < 0.17$ contains 484 asteroids with proper elements.

Our HCM run, performed in a single step in this region (see Paper I), finds there two small families: 6124 with 73 members, and 3561 with only 19.

However, if we definine first core families among the subpopulation with magnitude $H < 14.75$, we find a core family of (153) Hilda with only 14

members. This family is not recognized as significant in the single step HCM because the limit number for significance, in this case, would be set at 15 members. Since this candidate family was important and only marginally discarded, we have decided to use the two step procedure, at least to assess the situation. Then the second step, consisting in the attribution of fainter objects to the existing core families, gives a surprisingly small growth, namely the membership of family 153 increases only to 18 members. The conclusion is that a family of (153) Hilda can be considered to exist, but has a peculiar size distribution, strongly depleted in small size members; this is not due just to observational selection, since in the 3/2 resonance 52% of the asteroids with proper elements have $H > 14.75$.

The other families of (1911) Schubart, of (6124) Mecklenburg, not far from 153, and of (3561) Devine at lower a and e, are not affected at all, that is their membership is the same both with the one step and the two step procedure.

At levels of distance above the one which is prescribed by HCM, families 153 and 6124 merge at 70 m/s, 3561 merges at 120 m/s, thus forming a very large "super–Hilda" family (Paper I, Section 4.2). An even bigger extension of the Hilda family was proposed by Brož et al. (2011), with a limiting distance of 140 m/s; they also claim that it is a very ancient family, with an age estimated at about 4 Gy. This is a legitimate method to propose a family, although not a way to prove that it is statistically significant.

Thus we have decided to investigate the properties of the super-Hilda family, even if its significance cannot be proven by HCM.

The fact which is known about very ancient families is that they tend to erode: secular drifts due to Yarkovsky, chaotic escape routes, and collisional comminution must necessarily occur and affect all members, but in a size-dependent way. The non-gravitational perturbations typically are proportional to $1/D$, most resonances containing escape routes become accessible as a result of Yarkovsky secular drift, collisional lifetimes are shorter for smaller objects. Anyway, whatever the cause, ancient families dissipate by preferentially loosing the smaller members.

Thus it is possible that a super-Hilda family did exist, but is now so much depleted in small members that it cannot appear as a connected density contrast (which is statistically significant), but gets disconnected in three smaller islands. The slope of the size distribution of the 484 asteroids in the box cited above is $N(D) \sim 1/D^{-1.75}$, that is, extremely shallow.

If such a family existed, then it could still show a V-shape, in this case

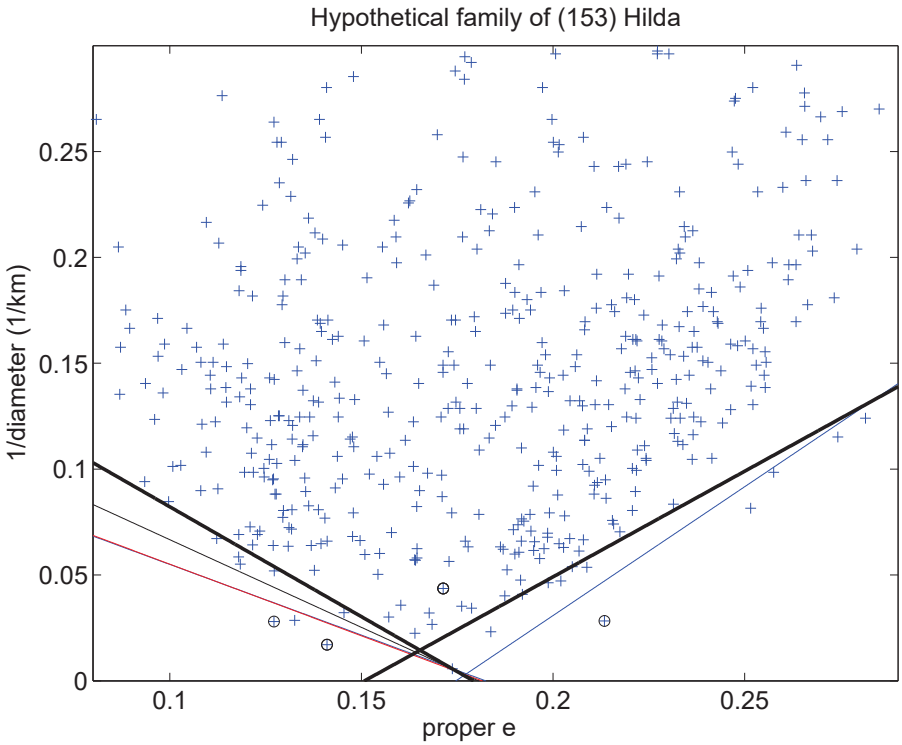

Figure 5: The V-shape for the super-family of (153) Hilda in the plane $(e, 1/D)$. Note that the V-shape is formed by comparatively large members, for the most part with $D > 10$ km.

of 3/2 resonance in the proper $(e, 1/D)$ plane. Indeed, Figure 5 does show a pronounced V-shape which can be used to compute an age. In the same time, neither of the small isolated groups does show any meaningful V-shape. The calibration of de/dt is obtained with exactly the same procedure as for family 1911, and with the similar result:

$$\frac{de}{dt} = 0.370 \cdot \frac{da}{dt}(NR) \ .$$

Note that for the drift in a due to the slope of the libration center the coefficient (w.r. to the drift which would occur outside the resonance) is also similar to the one for the family 1911: 0.020.

The slopes (see Table 4) are consistent. The Yarkovsky calibration converted in e is -1.83×10^{-10} in 1/y for the IN side and 1.99×10^{-10} for the

OUT side. The age estimate is $5,265 \pm 1,645$ for the IN side, $5,039 \pm 1,682$ for OUT, in My; the uncertainty is again dominated by the 0.3 relative uncertainty in calibration.

Of course the nominal value and higher values in the formally acceptable range are not possible, but the lowest part of the range of uncertainty gives legitimate ages, older than any other we have measured, and compatible with Brož et al. (2011) results. Such an old age estimate can indeed justify the very shallow size distribution; however, with the current number of identified members we cannot claim this is a strong confirmation of the age.

Note that, if this is really a very old family strongly depleted in small members, we should have here a rare case in which we can expect that future observations, extending the completeness limit to fainter objects, will *not* produce a significant increase of the number of family members, as opposite to the case of the large majority of asteroid families. This shall be futher discussed in Section 5.6

2.2. 1/1 resonance: the Trojans

The Jupiter Trojans dataset includes now 3357 objects surrounding L4 (the "Greek camp"), and 1663 surrounding L5 Lagrange point (the "Trojan camp"). The proper elements have been computed with the synthetic method described in Milani (1992, 1993), and are different in that the proper a is replaced by the semi-amplitude Δa of the libration in semimajor axis due to the 1/1 resonance[3]; the proper elements e and $\sin I$ are computed in the same way as in the main belt.

We have used, separately for the L4 and the L5 swarm, a single step HCM method, with the same metric of Zappalà et al. (1990, 1995), that is using for the differences in Δa the same 5/4 coefficient used for the differences in a in the main belt (anyway, the differences in Δa play a minor role due to the fact that their range of values is narrow: $0 < \Delta a < 0.17$ au).

The stalactite diagram for the L4 objects, obtained by using a value of $N_{lim} = 10$, is shown in Fig. 6. Since we found for the Quasi Random Level a value of 40 m/s, this means that families must be found at 30 m/s. The stalactite diagram for the L5 Trojan asteroids is shown in Fig. 7. The adopted

[3]To display the two swarms separately, but on the same planes as the main belt, in our visualizer at `http://hamilton.dm.unipi.it/astdys2/Plot/index.html`, we have used the values $a_J - \Delta a$ for L4, $a_J + \Delta a$ for L5.

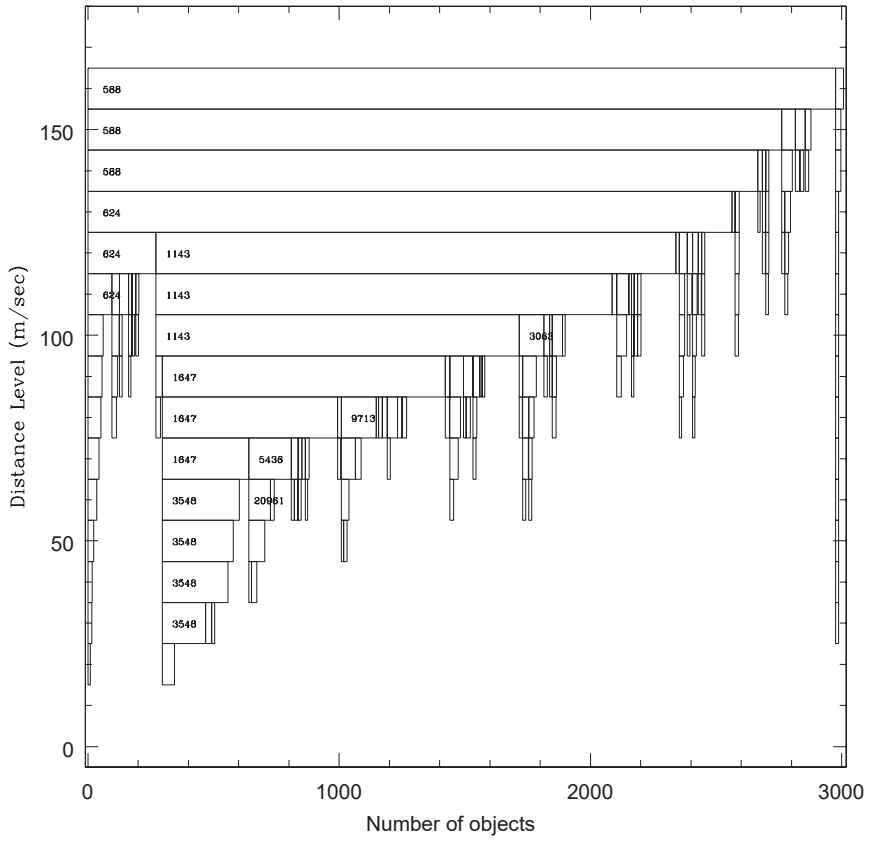

Figure 6: Stalactite diagram for the Trojans of the L4 swarm. The value of N_{lim} is 10. The distance level at which families are identified is 30 m/s.

value of N_{lim} for L5 is 7 and the QRL is found at 60 m/s. L5 families are therefore defined at 50 m/s.

By looking at the stalactite diagrams for L4 and L5, one sees a multitude of thin and in several cases very deep stalactites emerging from the bulk of the two populations. For some of them, mainly in L4, the unusual thing is just their thin and compact morphology.

This behaviour is not unexpected *a priori*. The dynamical environment in the Jupiter Trojan swarms is such that the usual mechanisms of dynamical dispersion of families at work in the main belt, including primarily the Yarkovsky effect, are much weaker here, even over long time scales.

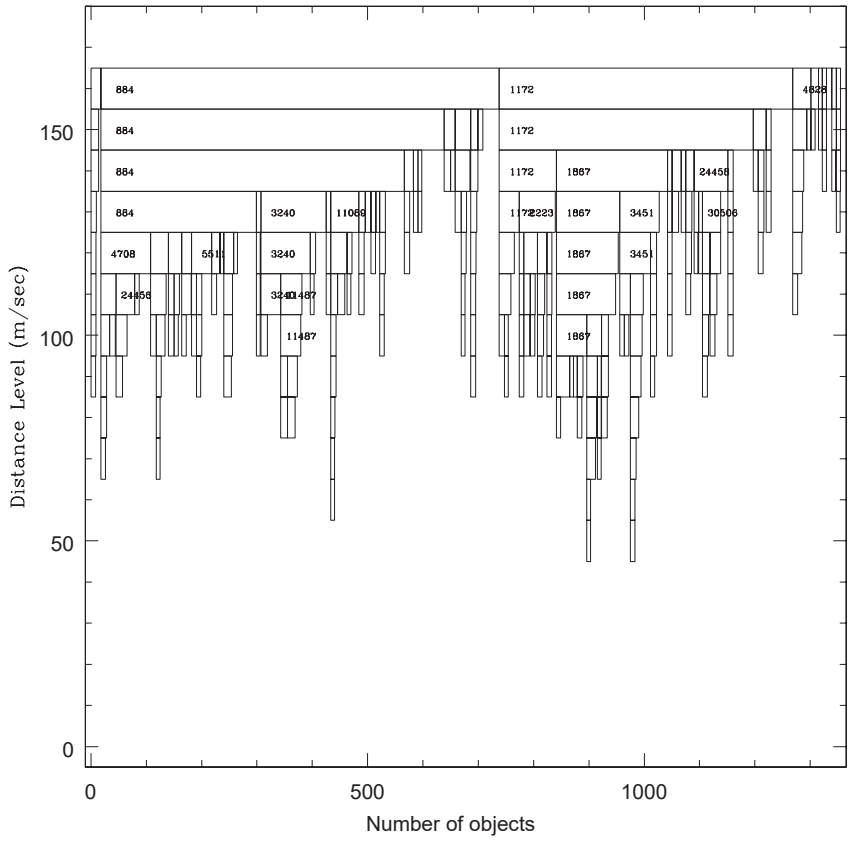

Figure 7: Stalactite diagram for the Trojans of the L5 swarm. The value of N_{lim} is 7. The distance level at which families are identified is 50 m/s.

As a consequence, swarms of fragments produced by collisions occurred in the Trojan swarms in very ancient epochs can be expected to survive until today with very little alterations of their orbital elements, whereas in the main belt identical groupings would tend to disperse and be dissipated over relatively short time scales. So, the general morphology of the stalactite diagrams shown in Figs. 6 and 7 can be interpreted in terms of very compact groups which may well be the survivors of events that occurred in very ancient times. The relatively small numbers of objects can also be a consequence of the fact that the smallest objects at this heliocentric distance have not yet been discovered.

It is also possible that for the Jupiter Trojan population our criteria for family acceptance, which have been defined to be applicable primarily to the case of main belt asteroids, could be overly severe. In other words, we cannot rule out the possibility that some, relatively deep stalactites that do not satisfy our criteria to be accepted as families, might still be the remnants of ancient collisional events.

Unfortunately, one of the major tools we have at disposal to test similar hypotheses among main belt astreroids, namely the evidence coming from spectroscopic and/or polarimetric evidence, are much less powerful a priori when applied to the Jupiter Trojans, which are quite homogeneous in terms of spectral properties and sufficiently faint to be a challenge for polarimetric measurements.

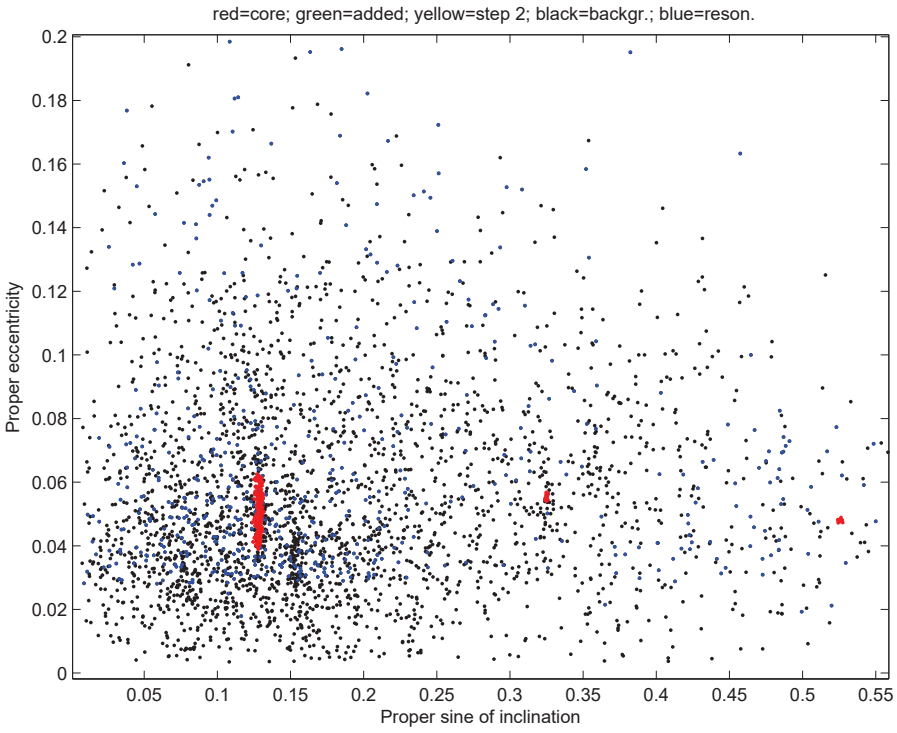

Figure 8: Proper eccetricity versus sine of inclination plot for the L4 Jupiter Trojan swarm.

The Eurybates family

Somewhat less compact, but by far the most populous group in the L4 Trojan swarm is the family of (3548) Eurybates. It includes 172 members, 41 of them being multi-opposition objects.

Strictly linked to Eurybates are 8060 and 222861, two small groupings, consisting of 25 members, including 5 multi-opposition objects, and 11 members (3 multi-opposition), respectively. These families are very close to Eurybates, and join it already at the level of 40 m/s, just 10 m/s above the level for statistical significance.

The family of (3548) Eurybates is located in the tip of a larger stalactite branch well visible in Fig. 6. This also corresponds to the most evident grouping with proper sine of inclination about 0.13 and proper eccentricity around 0.05 in the plot shown in Fig. 8.

We have used the same calibration method of Section 2.1 to get the right order of magnitudes of the secular effects in all proper elements. On Δa the secular effect of Yarkovsky is $\sim 10^{-5}$ of the corresponding effect in a outside the 1/1 resonance, thus dispersion in Δa is negligible even over the age of the Solar System. For proper e the ratio of de/dt with the non-resonant da/dt is 3×10^{-3}, for proper $\sin I$ it is 4.6×10^{-3}. Thus, although it is possible to plot the family members in either a $(e, 1/D)$ plane or in a $(\sin I, 1/D)$ plane and measure slopes of the V-shapes, the values of the ages which would result from the hypothesis that these V-shapes describe a Yarkovsky effect are by far too large: the smallest one resulting from the use of $(\sin I, 1/D)$ is 14 Gy, little more than the age of the universe.

This implies that the distribution of proper elements of the family members is essentially only due to the original distribution of relative velocities of the fragments, with very minor contribution from any non-gravitational perturbation. Thus we cannot estimate the ages of the Trojan families, but we can assess the distribution of the original velocities, something which is not possible in the asteroid main belt (apart from the case of recent families).

As a check of this approach, we have computed the standard deviation of the proper elements of the members of 3548, and found 0.0048 for proper e, 0.0015 for proper $\sin I$ and 0.0107 au for Δa, corresponding to relative velocities after escaping from the gravitational well of the parent body of 62, 20 and 13 m/s, respectively. The parent body can be estimated from the family volume to have had $D = 93$ km, thus the escape velocity can be roughly estimated (we have very poor density data) at about 100 m/s. Thus

the values of the relative velocities obtained from the present values of the proper elements are fully compatible with an original velocity field.

High inclination Trojan families

The families of (624) Hektor and of (9799) 1996 RJ, with 15 objects (6 multiopposition) and 13 (6 multi-opposition), respectively, correspond to two extremely compact, deep and well isolated stalactite branches which are evident at the left and rigth ends of the stalactite diagram shown in Fig. 6.

Both families have relatively high inclination ($\sin(I) \simeq 0.33$ for 624, $\sin(I) \simeq 0.53$ for 9799). Their extremely compact structure is clearly visible in the sine of inclination - eccentricity plot (Fig. 8) where they correspond to very compact clusters ressembling big blots in the middle-right part of the Figure, at proper eccentricity values slightly above and slightly below 0.05, respectively.

By the same argument used for 3548, the distributions of proper elements should reflect the original field of relative velocities after the exit from the sphere of influence of the parent body: both these families are of cratering type. (624) Hector is a very large, oddly shaped body (suspect contact binary) with a satellite. The RMS of proper elements differences, with respect to those of the parent body (624), are 0.0042 au for Δa, 0.0009 for e, 0.0006 for $\sin I$, corresponding to velocities after escape of $5, 11$ and 8 m/s respectively. These numbers are so much smaller than the escape velocity from (624) Hektor, which is about 130 m/s, to point out to a marginal escape from a cratering event, possibly the same resulting in the formation of a satellite and also of the contact binary.

The same argument can be applied to the family of (9799) 1996 RJ, which is also of cratering type, with RMS of differences in proper elements corresponding to $4, 6$, and 15 m/s for $\Delta a, e$, and $\sin I$, respectively. All the three examples analysed above appear to confirm that the Trojan asteroid families are **fossil** families, frozen at their proper elements which are essentially determined by the original ejection velocity field. On the other hand, these velocity fields are remarkably different in cratering vs. fragmentation cases.

Looking at the same Figure, we also note that few other, less compact groupings are present, but they do not correspond to acceptable families according to our HCM criteria. As mentioned above, this might be a consequence of applying overly conservative criteria of identification in a region in which families tend to last over very long timescales without relevant erosion. Some of these groups might "grow" in the future, and become acceptable,

when the magnitude completeness limit for the Trojans will improve. A good example may become a family of (2148) Epeios, proposed by Vinogradova (2015), which can be found by relaxing the HCM significance criteria.

2.3. 2/1 resonance: the Griqua region

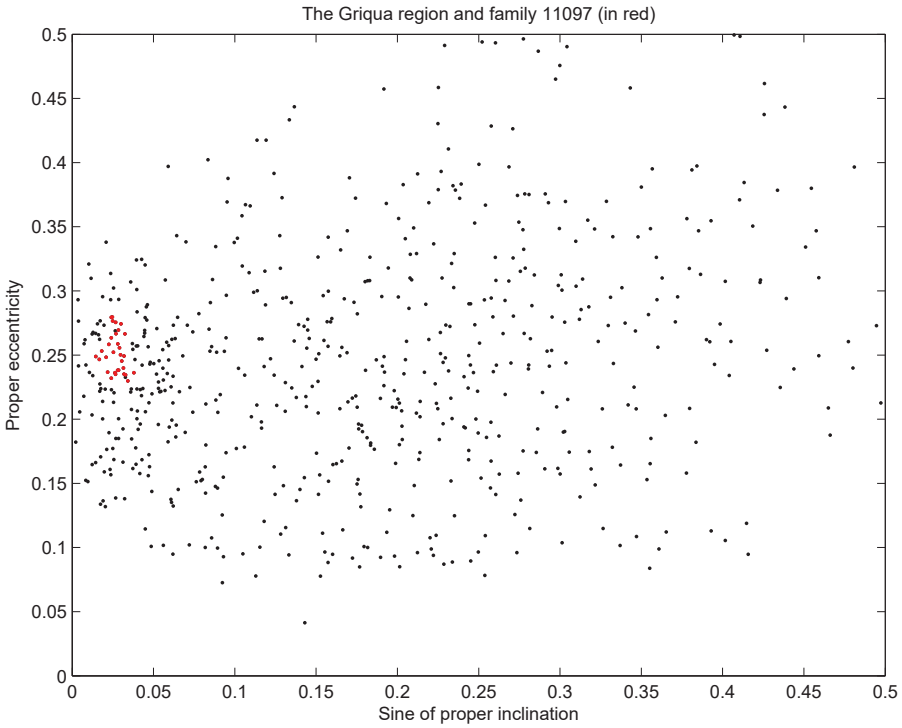

Figure 9: The Griqua region projected on the proper $(\sin I, e)$ plane. The red points are the family of (11097) 1994 UD1.

The Griquas are a comparatively small (649 asteroids) population of asteroids confined in the 2/1 mean motion resonance with Jupiter, in a tight range of "semi-proper" semimajor axis: $3.26 < a < 3.28$. By the same argument used for Hildas, the computation of true resonant proper elements is not necessary. Griquas are fairly spread in proper eccentricity and sine of inclination, between 0 and 0.55 and between 0 and 0.65, respectively, see Figure 9 [4].

[4]The name of this population is taken from the lowest-numbered asteroid present in

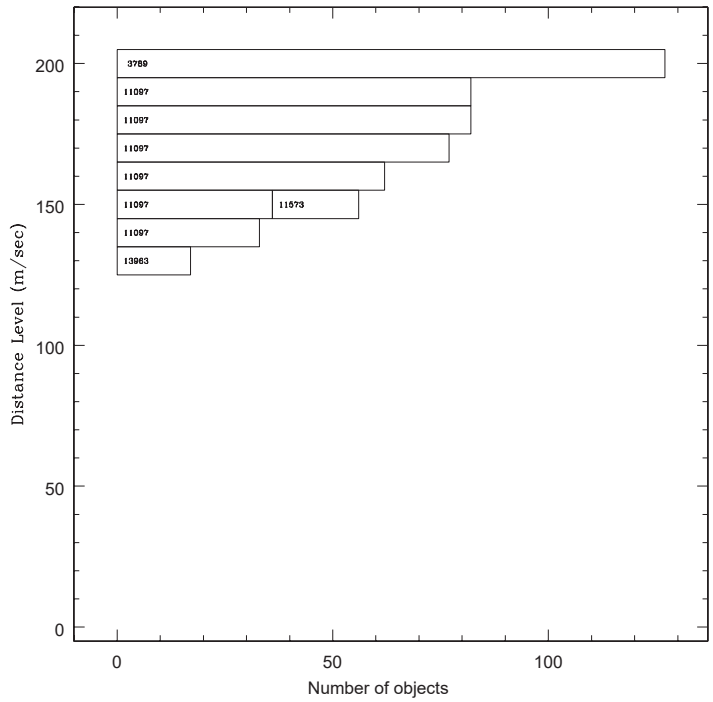

Figure 10: Stalactite diagram for the Griquas population. The minimum number of objects to form an acceptable group is $N_{lim} = 16$. The distance level at which families are identified is 140 m/s.

The classification of Paper I did not find any statistically significant family in this region. However, the statistics might have been distorted by merging the sparsely populated 2/1 region with the very populated Zone 4, with a above the 5/2 gap. Thus we have rerun a dedicated classification for the Griquas only: of course the quasi-random background became sparse, thus allowing to detect smaller families.

In this region, we adopt for N_{lim} a value of 16. The stalactite diagram is shown in Fig. 10. The Quasi Random Level for the Griquas is found to be $QRL = 150$ m/s, implying that the distance level to identify families is 140 m/s. Only one such group is present, the 11097 family, which has 33

this region, (1326) Griqua.

members, including 2 multiopposition objects. It corresponds to a group that is apparent in Figure 9, where it is located at very low proper inclination. This is a small family, which deserves further study, also to be confirmed by observation of a homogenous composition.

3. Families affected by secular resonances

There are in our classification five families with enough membership to be suitable for age estimation, but affected in significant way by the secular resonances, in which either all or a good portion of the members are locked; for a map of the secular resonances in the main belt, see Milani and Knežević (1994)[Fig. 7-11]. To provide a theory of the long term dynamical evolution of asteroids affected by both secular resonances and Yarkovsky effect is beyond the scope of this paper; some cases have been discussed in the literature (Bottke et al., 2001; Vokrouhlický et al., 2006).

Our goal for this paper is just to estimate ages, thus we are going to use an empirical approach very similar to the one we have used for the Hildas: by numerical integration we perform a calibration for the Yarkovsky effect inside the resonance versus the Yarkovsky effect which would occur to the same asteroid if the resonance was not there. In this way we solve all five cases, three with either all or a good portion of the members locked in the resonance (families 5, 363, 945), and two (families 283, 686) which have only a minor portion of members affected by a secular resonance, such that the V-shape in $(a, 1/D)$ can not change by the action of the resonance.

3.1. The Astraea family

To understand the shape in proper elements space of the family of (5) Astraea is a complex problem, both because almost all its members are locked in the $g + g5 - 2\,g_6$ nonlinear secular resonance (with values $|g + g5 - 2\,g_6| < 0.5$ arcsec/y), and because the proper e has a large spread, up to 0.236, a value such that it must be due to a large number of mean motion resonances affecting the stability of the proper elements over very long time spans. Note that many of these mean motion resonances are with inner planets, thus they are not included in the computation of the proper elements for the asteroids of the outer main belt ($a > 2.5$ au) Knežević and Milani (2000). In the case of the family 5, with lowest value of proper $a = 2.55$ au and with comparatively high eccentricity, to include the inner planets in the dynamical model, as in Knežević and Milani (2003), could improve the results.

Physical observations available for this family are few, because it originated by a cratering, thus has especially small members: 77% of the members have $D < 2$ km. WISE albedo data (Masiero et al., 2011) with nominal $S/N > 3$ are available for only 6.5% of the family members; out of these, 31% of the albedo values are < 0.1, that is they indicate interlopers, since (5) has IRAS albedo (Tedesco et al., 2002) 0.227 ± 0.027. This fraction of interlopers is somewhat high, but not extraordinarily so (Migliorini et al., 1995; Radović and Novaković, 2014): it could have been affected by the "compression" resulting from the standard computation of proper elements which does not specifically account for the secular resonance. Because this compression applies to both the real family family and the background, this can explain a larger fraction of interlopers. Anyway, this comparatively large fraction of interlopers is a fact and we need to take it into account in our age estimation procedure.

If we analyse the V-shape in the $(a, 1/D)$ plane (Figure 11) we see that the computations of the slope are possible, although the IN side is affected by a group of four members too large for their position, near the inner edge of the family: e.g., (4700) Carusi has an estimated $D > 8$ km. Near the center of the family, (1044) Teutonia has an IRAS estimated $D = 15$ km, which is incompatible with the cratering origin of the family. Moreover, the fit for the IN side was very poor, to the point that the inverse slope was barely significant.

We have therefore decided to discard a priori 4 interlopers, marked with a red circle in Figure 11; then also (1044) Teutonia was automatically discarded as outlier in the fit. After these removals, the family contains no member with $D > 7$ km and the fit has been much improved, being compatible with a single collision origin and with a similar uncertainty on the two sides. Our choice of four members interpreted as interlopers is plausible also because of the large fraction of interlopers in general in the family.

Before interpreting the inverse slopes of the V-shape as measures of age, we need to perform a calibration of the Yarkovsky effect taking specifically into account the dynamical environment of the family. For this purpose we have performed a numerical integration for 10 My, with inner planets included, for 200 clones of (5) Astraea. The right hand side of the equations of motion included Yarkovsky accelerations corresponding, for a non-resonant objects, to values of secular da/dt in the range $-3.6 \times 10^{-9} < da/dt(NR) < 3.6 \times 10^{-9}$ au/y. After computing for each clone 9 sets of proper elements (as in Section 2.1), we computed for each clone the "resonant" $da/dt(RES)$

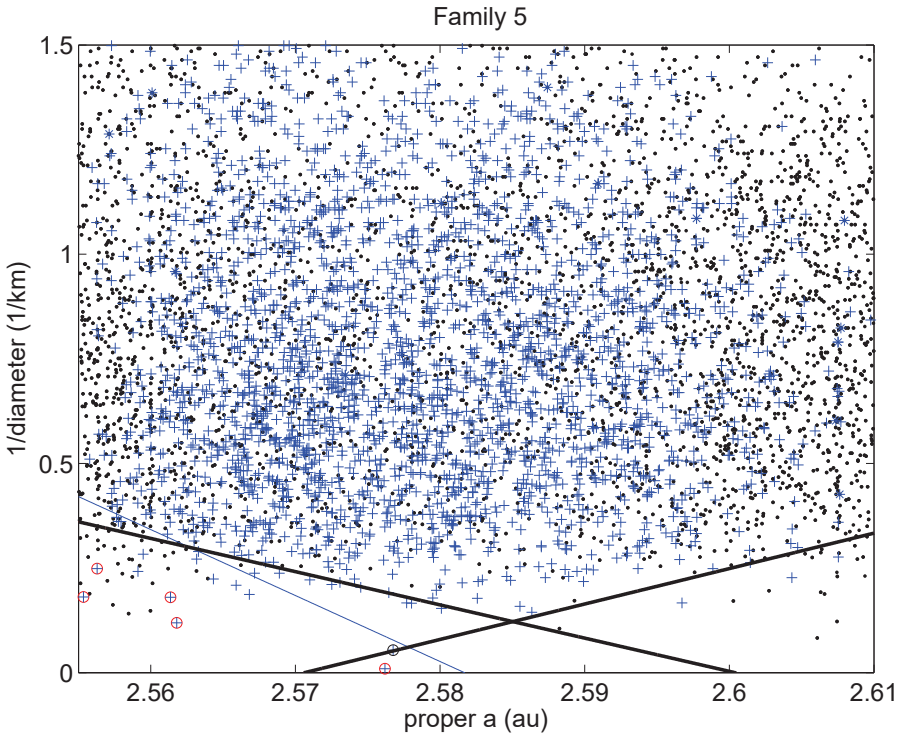

Figure 11: V-shape of the family of (5) Astraea, whose members are locked in the $g + g_5 - 2\,g_6$ nonlinear secular resonance. (5) Astrea is not included in the slope fit because the family is of cratering type. Blue crosses are family members, black dots are background objects.

drift, then plotted the result in Figure 12 with the fit to a line which has slope 1.008. In other words:

$$\frac{da}{dt}(RES) = 1.008 \cdot \frac{da}{dt}(NR) \ ;$$

meaning that the amount of secular change in proper a due to Yarkovsky is not significantly affected by the secular resonance.

We can therefore conclude on the age as reported in Table 8: 339 ± 104 for the IN side, and 319 ± 98 for OUT, in My; the age of family 5 is old, but far from ancient, and represents another very good example of cratering, significantly younger than Vesta.

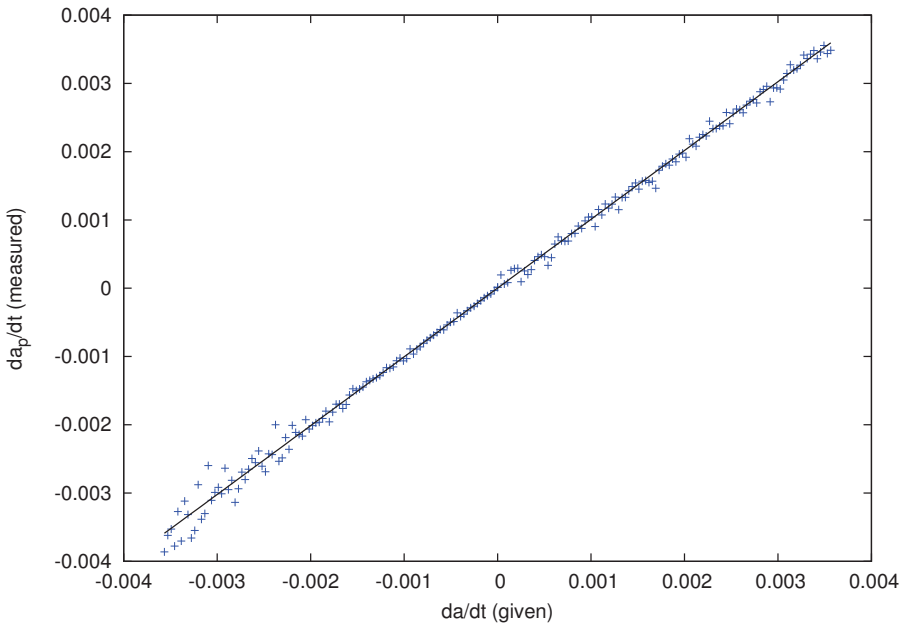

Figure 12: Yarkovsky calibration for the family of (5) Astraea. Slightly larger dispersion of the fit points at the far negative side of the regression line is due to the mean motion resonances.

3.2. The Padua family

Our classification includes a dynamical family of (110) Lydia, whith almost all members locked in the $g + g_5 - 2\,g_6$ nonlinear secular resonance (the same as for family 5). However, (110) has WISE albedo $= 0.17 \pm 0.04$ while 90% of the members having WISE data (with $S/N > 3$) have albedo < 0.1. Thus (110) Lydia is a very likely interloper and the family namesake should be (363) Padua. We applied this change in the tables, starting from Table 5.

The V-shape of Figure 13, besides confirming the need to remove (110) from the family list, gives good fits for the inverse slopes with compatible values, suggesting a single age[5].

[5]The slopes of the V-shape of family 1726 are -0.199 ± 0.028 on the IN side and 0.192 ± 0.025 on the OUT side, thus the value obtained for family 363 implies that the two families are not from the same collision, thus confirming the choice made in Paper IV of not merging these two.

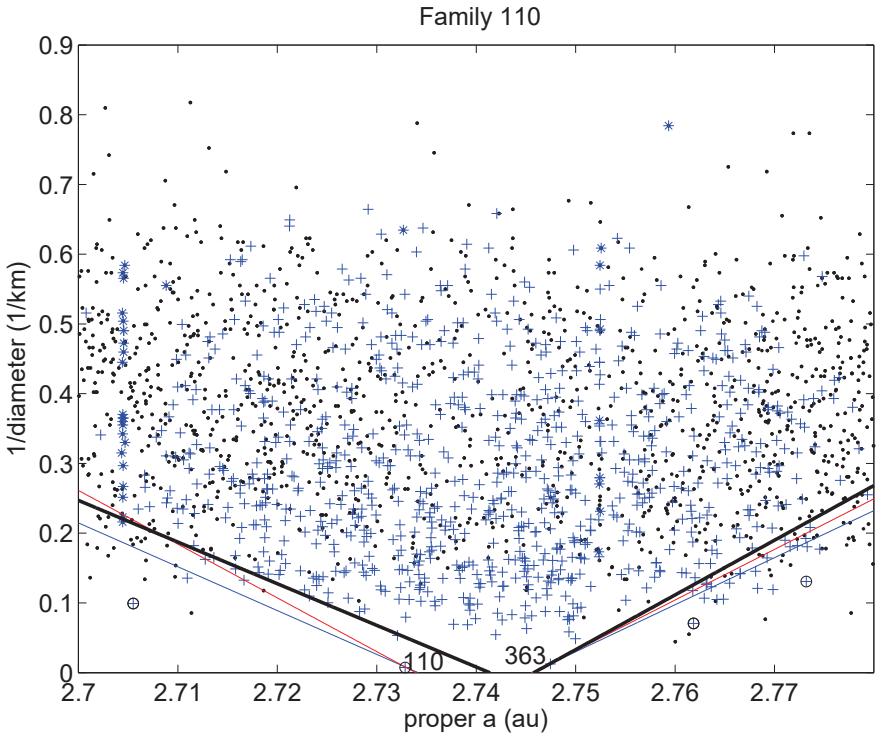

Figure 13: V-shape of the family of (363) Padua; note that (110) Lydia is also an outlier in the slope fit, confirming its exclusion from the collisional family by physical properties.

In the same way as we did for family 5, we have computed[6] the calibration for the secular $da/dt(RES)$ inside the resonance as a function of the one for $da/dt(NR)$ outside the resonance, and we got a figure very much like Figure 12, with a fit slope of 0.985 and some noise for positive values of $da/dt(NR)$, presumably due to a number of mean motion resonances, including 3J-1S-1A. We do not think that the difference between the calibration 1.006 of the previous case and this one is significant, anyway it gives a negligible contribution to the relative uncertainty of the calibration.

After calibration, the ages reported in Table 8 indicate a family at the low end of the "old" range: 284 ± 73 for the IN, and 219 ± 48 for the OUT

[6]Given the larger value of proper a, we have performed the 10 My numerical integration with a model including this time only the outer planets.

side, in My, compatible with a single collisional origin of fragmentation type, although with a largest remnant (363) containing as much as 75% of the family volume.

3.3. The Barcelona family

The family of (945) Barcelona has about 2/3 of the members (the portion of the family with proper $e > 0.23$) strongly affected by the resonance between the perihelion precession of the asteroid g and the one of Jupiter g_5, with $|g - g_5| < 2$ arcsec/y. Another unidentified nonlinear secular resonance is also relevant for the dynamics of most members.

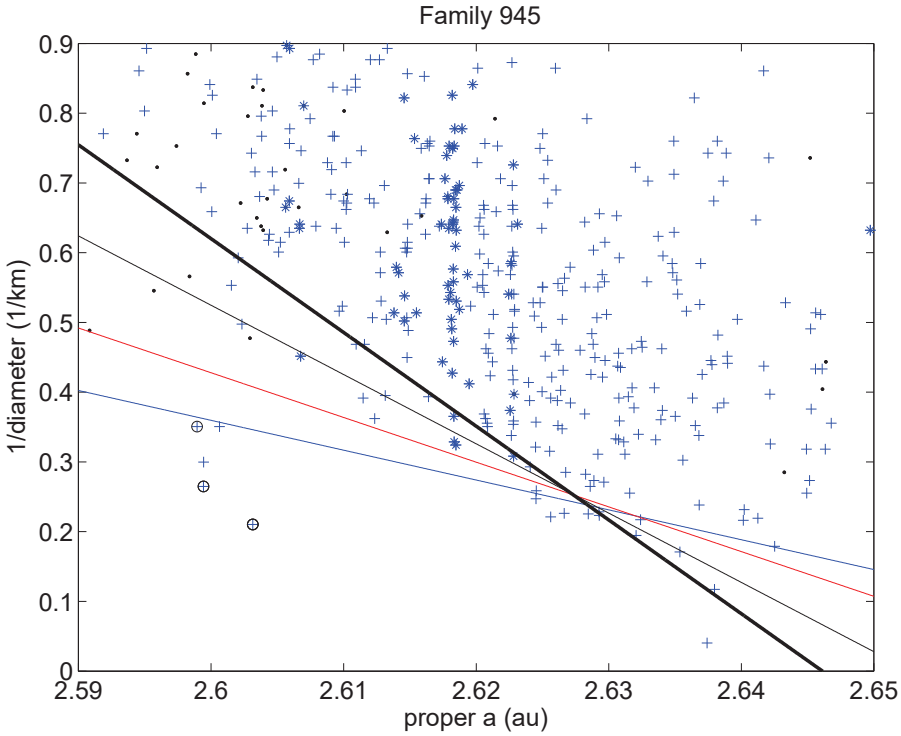

Figure 14: One-sided V-shape of the family of (945) Barcelona. The gap on the right, where the family terminates on the OUT side, corresponds to the 11/4 J resonance at $a \simeq 2.649$.

The family is bound on the OUT side by the 11/4 mean resonance with Jupiter, thus its V-shape (Figure 14) has only the IN side. The IN side fit

is good, with some outliers, allowing to estimate the inverse slope with good accuracy.

We confirm our approach of a purely numerical calibration of $da/dt(RES)$, not only because a theory of the evolution under Yarkovsky effect plus two overlapping secular resonances is out of the scope of the present paper, but as it also appears exceedingly difficult. The same calibration as in the case of family 363 gives a slope of $da/dt(RES)$ versus $da/dt(NR)$ of 1.046. The plot shows much more noise than in the previous two cases, some of which is associated with the 11/4 resonance: this noise does not affect the family which has been depleted by the resonance. Still our conclusion is the same: the effect of the secular resonance on the rate of Yarkovsky is small, to the point of not being significant with respect to the relative calibration uncertainty.

The age of 203 ± 56 My is again at the low end of the "old" range, the family is of fragmentation type but with a comparatively large remnant (945) with 73% of the family volume.

3.4. The Gersuind family

Our classification contains a dynamical family 194, with 408 members. However, the family namesake (194) Prokne has albedo 0.052 ± 0.015 (WISE) thus it does not belong to the family, which, after removal of members with albedo < 0.08 and > 0.25, has a mean albedo 0.145 ± 0.037 . The low albedo of (194) has been confirmed with recent polarimetric measurements by Devogele et al. (2016).

After the removal of such a large interloper, (686) Gersuind remains the lowest numbered member, with albedo 0.142 ± 0.037, thus the family has to be called family 686; we applied this change in the tables, starting from Table 5. A family of (686) Gersuind, without (194), had already been proposed by Novaković et al. (2011).

As afore mentioned, this family is only partially affected by the $s - s6 - g5 + g6$ nonlinear secular resonance, with only some 14% of members in the OUT side having the corresponding frequency $|s - s6 - g5 + g6| < 0.5$ arcsec/y.

The V-shape of the family 686 (Figure 15), with (194) and other members with incompatible albedo removed, still results in a poor fit for the IN side, with $1/S = -0.569 \pm 0.322$, but in a better one for the OUT side 0.534 ± 0.138. After calibration, which yielded regression line slope of 1.003, the estimated ages are 1490 ± 843 and 1436 ± 469 My, with the OUT value much more significant.

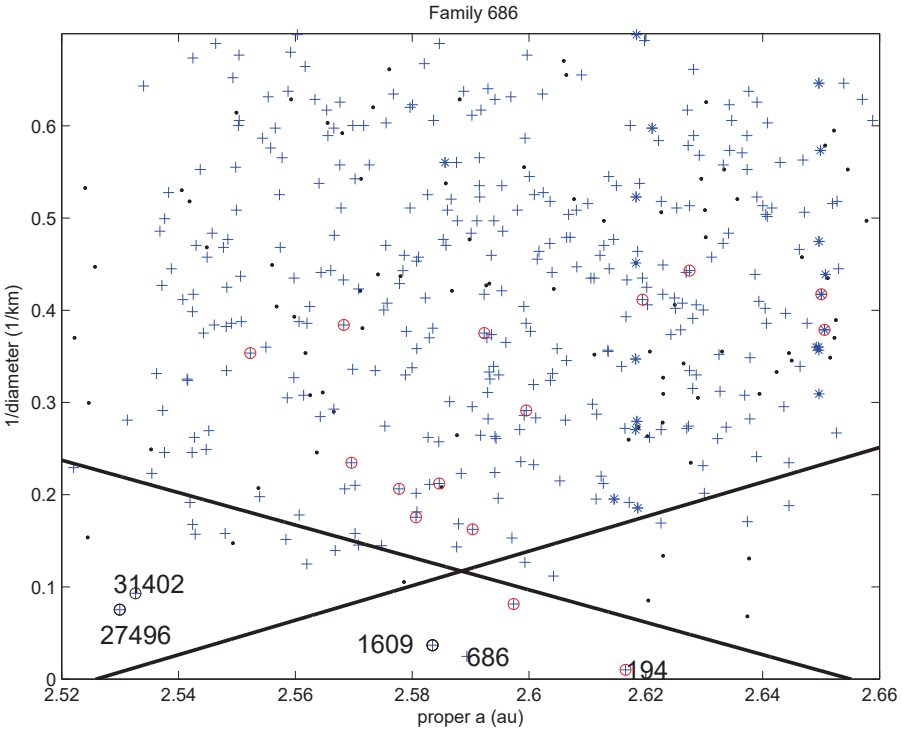

Figure 15: V-shape of the family of (686) Gersuind. The asteroids marked with a red circle are interlopers discarded by albedo, the ones with a black circle are removed from the fit as outliers.

Note that the members (1609), (27496) and (31402) are removed as outliers from the slope fit: since there are no albedo data their status as interlopers remains to be confirmed.

3.5. The Emma family

The family of (283) Emma contains dark asteroids, with few known higher albedo interlopers: the mean WISE albedo is ~ 0.05, (283) itself has an IRAS albedo 0.026. A small fraction (about 8%) of its members are affected by the nonlinear secular resonance $g + s - g6 - s6$, which opens a kind of gap between two parts of the family, well visible in the projection on the proper $(a, \sin I)$ plane, for low values of a.

The V-shape (Figure 16) results in a good fit on the IN side with $1/S = -0.165 \pm 0.019$, thus it does not appear to be much affected by the secular resonance. To the contrary, on the OUT side the fit is poor: 0.355 ± 0.112.

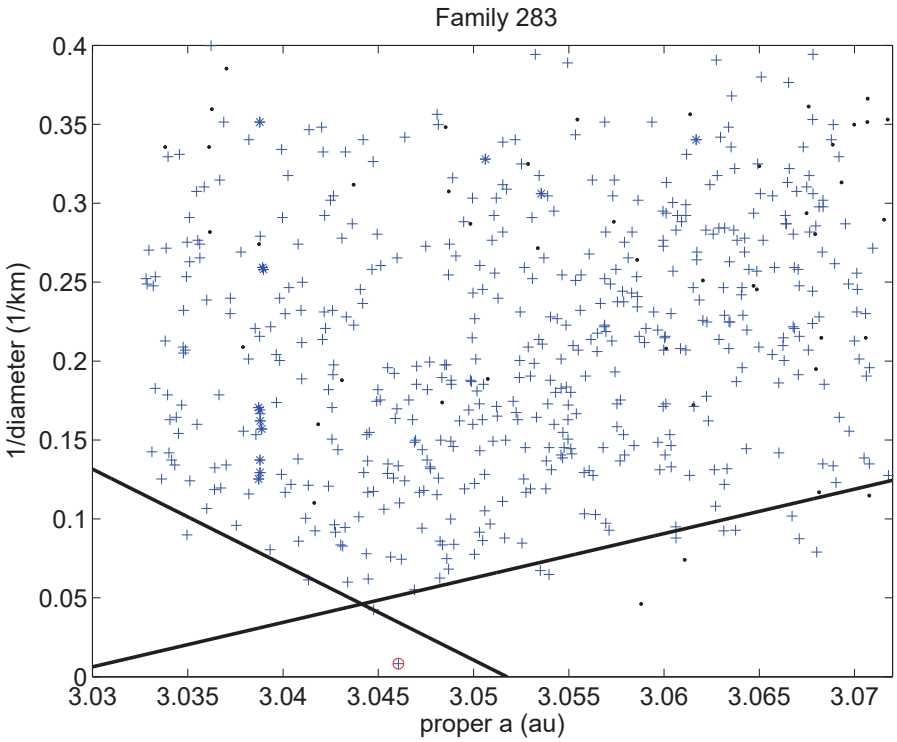

Figure 16: V-shape of the family of (283) Emma; the two slopes are ostensibly different. Note that the family is of cratering type, thus the parent body (283) Emma is excluded from the fit (marked with red circle), as well as from calibration.

After calibration performed on the second largest family member (32931) Ferioli (regression line slope 1.010), the age estimates are 290 ± 67 on IN side, and 628 ± 234 My on the OUT side. The family is of cratering type: assuming same albedo for all, the volume of the family members without (283) is about 9% of the total. Thus the occurence of two separate cratering events is a reasonable hypothesis, which is consistent with a double jet shape as shown in the proper $(a, \sin I)$ projection.

3.6. The Phocaea family

The family of (25) Phocaea has a one-sided V-shape in the $(a, 1/D)$ plane (Figure 17), with (25) at the high a end. The missing part of the V-shape is due to the resonances bordering the stable region, including the 3/1 J. The region contains about $4,000$ asteroids, while the dynamical family 25 contains

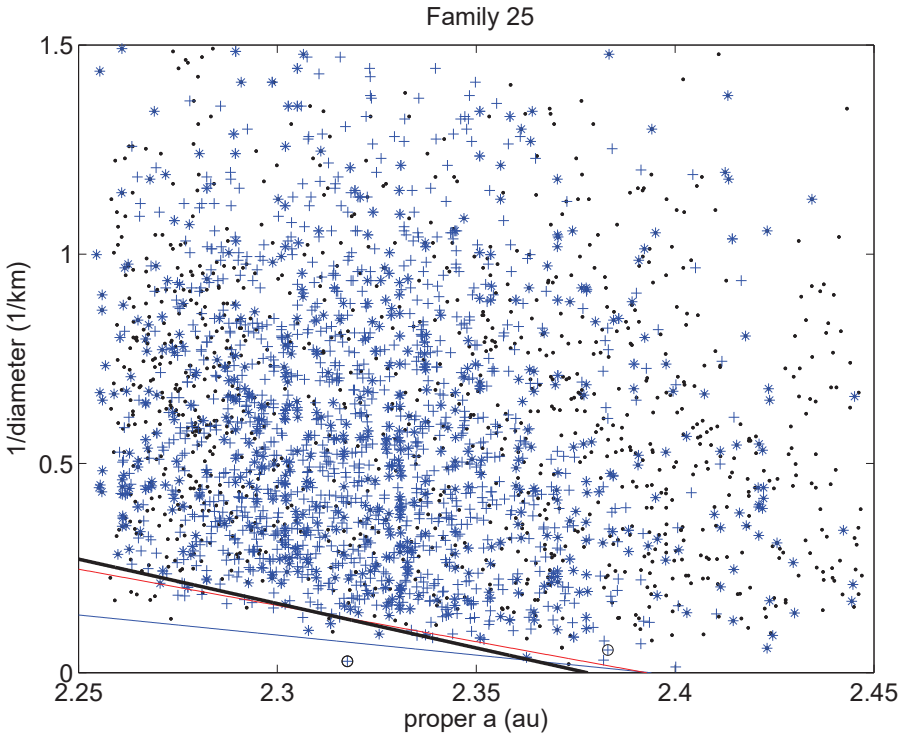

Figure 17: V-shape of the family of (25) Phocaea. The circled cross is (326) which is an outlier for the V-shape fit as well as an inteloper because of its low albedo.

only $1,405$ of these, thus it represents a substructure whith distinctive number density inside the stability region. The fit gives $1/S = -0.471 \pm 0.047$.

The only problem with the shape of the family as shown in Figure 17 is that there is obviously a lack of family members near the value of proper a of (25) Phocea, which occurs before the high a end of the stability region. This might be interpreted as a YORP induced central gap (Paolicchi and Knežević, 2016).

1/3 of the family members are affected by a nonlinear secular resonance: they have $|g - s - g_6 + s_6| < 0.5$ arcsec/y. This fraction is relevant for the age computation because it may affect the side of the V-shape, thus we need calibration, which has been done in the same way by using clones of (323) Brucia (which is locked in the resonance), but only with negative Yarkovsky drift in proper a. The slope of the $da/dt(RES)$ with respect to the one outside the resonance was found to be 0.977, thus once more the calibration

does not need to take into account the resonance. Thus the calibrated age is 1187 ± 319 My, an ancient family according to the terminology introduced in Paper III.

4. Irregular families

By irregular families we mean dynamical families with internal structures that cannot be interpreted as a simple, single collisional family; this either prevents the computation of an age, or results in an age which refers to only a portion of the dynamical family. In some cases, an interpretation as two or more collisional families (partially overlapping) is possible, e.g., Vesta, Eunomia, Agnia. Alternatively, this apparent complexity could be due to a number of comparatively large interlopers. In other cases the shape of the family can have different, even more peculiar interpretations. In this section we shall propose a solution, including an age estimation, for one of the previously unsolved cases. As explained above, family of (283) Emma obviously fits to this class, but being also crossed by the secular resonance, we preferred to deal with it in Section 3.

4.1. The Adeona family

The family of (145) Adeona has a peculiar shape in the proper a, $1/D$ plane which appears different from the standard V-shape. There appears to be a common V-shape for a narrow range of values, roughly $2.63 < a < 2.70$, while the portion of the family for $2.57 < a < 2.62$ is much less dense and does not appear to be delimited by the main V-shape.

The histogram of number density as a function of proper a (see Figure 19) shows a sharp decline of dynamical family membership in the region with a below the three 3-body resonances, 4J-3S-1A at $a \sim 2.623$, 2J+2S-1A at $a \sim 2.615$ (Smirnov and Shevchenko (2013)), and another not identified one at $a \sim 2.618$ au.

This complex structure can have different interpretations: the portion of the dynamical family for $a < 2.615$ could be another, smaller family with lower number density. The same portion could also be a continuation of the family of (145) Adeona with decreased number density, since a large fraction of members could have been removed by the resonances: then the largest members in the low a region should be interlopers.

There is, however, a certain indication from physical observations: the dynamical family contains mostly dark asteroids - 94% with WISE albedo

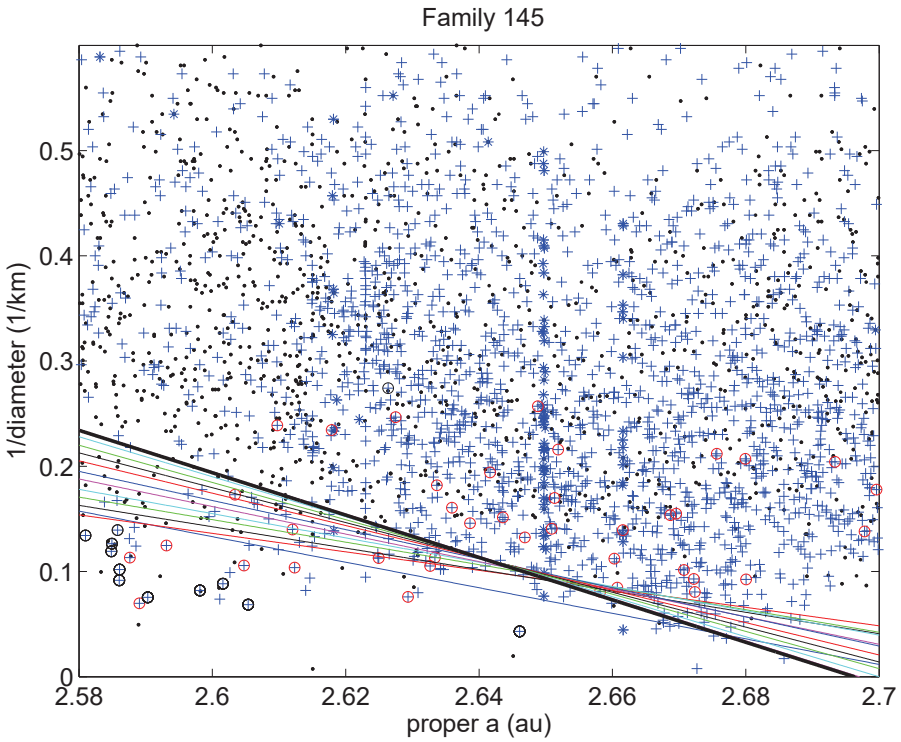

Figure 18: One-sided V-shape of the family of (145) Adeona. The crosses with red circles correspond to interlopers based on physical observations of either albedo or color indices; the ones with black circles are outliers removed from the V-shape fit. The colored lines represent intermediate steps in the fit, due to a large number of outliers being removed in several iterations.

< 0.1 - with a few interlopers. The unexplained group of comparatively large members for $a < 2.62$ au contains a fair fraction of interlopers, characterized either by albedo > 0.1 or by the color index $a^* > 0$ (see the circled crosses in Figure 18).

If we just fit the data to a V-shape with the IN side only, we get an inverse slope $1/S = -0.497 \pm 0.058$. As shown in Figure 18, the number of outliers removed to obtain this fit is substantial, on top of the interlopers removed by physical observations. The lack of the OUT side can be due to the strong 8/3J resonance at $a \sim 2.704$ au where the family abruptly ends up. Thus the age can be estimated as 794 ± 194 My. As discussed in Section 5, this result needs to be confirmed by showing that to discard that many data points is

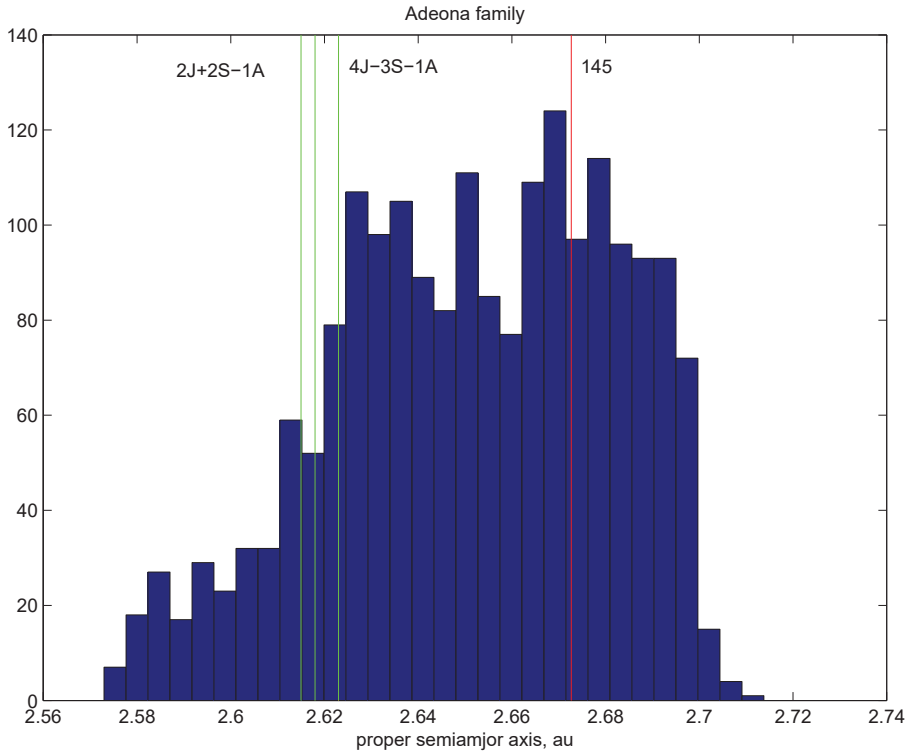

Figure 19: Histogram of proper a for the family of (145) Adeona. The region of higher number density ranges from about 2.62 to 2.70, and contains (145) Adeona itself, marked by the red line. The region of lower number density corresponds to values of a below the three resonances marked by the green lines.

justified.

5. Observational tests of families

As described in Paper I, our approach to asteroid family analysis is based on using the proper elements data first to identify the families, then adding the absolute magnitude data (with complementary information from the statistics of the albedo data in each family) to estimate ages, then use other available physical data to refine the results, e.g., identifying complex familes with more than one collision and interlopers which can deteriorate some age estimates. However, in many cases we do not have enough physical data to solve the problem. Thus we discuss in the following several open problems for

which dedicated observations of asteroid physical properties could decisively contribute to the solution of some interesting problems.

5.1. The Hertha complex

The single dynamical family of (135) Hertha has been known for a long time to include multiple collisional families, overlapping in the proper elements space (Cellino et al., 2001, 2002). However, we have been able to compute only one age (Paper IV), for the subfamily of (650) Amalasuntha, which is partly separate in the (a, e) plane and also distinguished by low albedo and other physical properties typical of the C taxonomic complex. A possible splitting of the low-albedo component of the Hertha complex in more than one group, in particular the presence of an independent Eulalia family (Walsh et al., 2013; Dykhuis and Greenberg, 2015) has not been supported by recent spectroscopic observations by De León et al. (2016).

The complementary "bright" subfamily does not have a recognizable V-shape. The recently proposed Hertha 1 and 2 families (Dykhuis and Greenberg, 2015) were found by using color index separation based on SDSS parameters. The presence of three density contrast features is confirmed by our last classification, in which family 135 has a total of $15,442$ members[7]; however, the location of the two "bright" subfamilies does not correspond precisely to what was proposed by Dykhuis and Greenberg (2015). Moreover, the role of (135) Hertha as (core of) parent body has not been established.

Targeted physical observations of several members of family 135, by selecting asteroids in such a way that they belong to the separate density features, could provide a robust collisional interpretation.

5.2. The Baptistina complex

For the complex of three dynamical families of (298) Baptistina, (883) Matterania, and (2076) Levin (see Figure 20) we do not have a collisional interpretation. The three families have few intersections [8] in the current classification, but we do not see any way to model them as the result of a single collision. Even an interpretation in terms of two collisions does not solve all the problems. The physical data (see Figure 21 for the SDSS data) only

[7]See the proper (a, e) projection of family 135 on our family visualizer at http://hamilton.dm.unipi.it/astdys2/Plot/index.html; note the bimodality of the bright component shown by the number density histogram on the right border of the plot.

[8]By intersection we mean members in common, see Papers I and II.

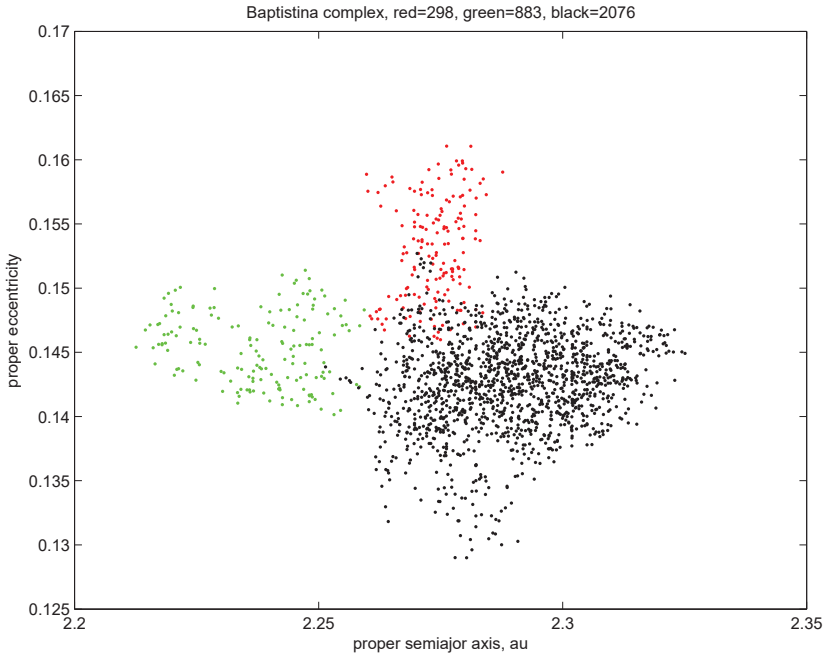

Figure 20: Distribution in the plane of proper (a, e) of the members of families 298 (red), 883 (green), 2076 (black). There are currently 2 intersections between 298 and 2076 and 1 intersection between 883 and 2076. The projections on other proper element planes $(a, \sin I)$ and $(e, \sin I)$ show a similar complexity.

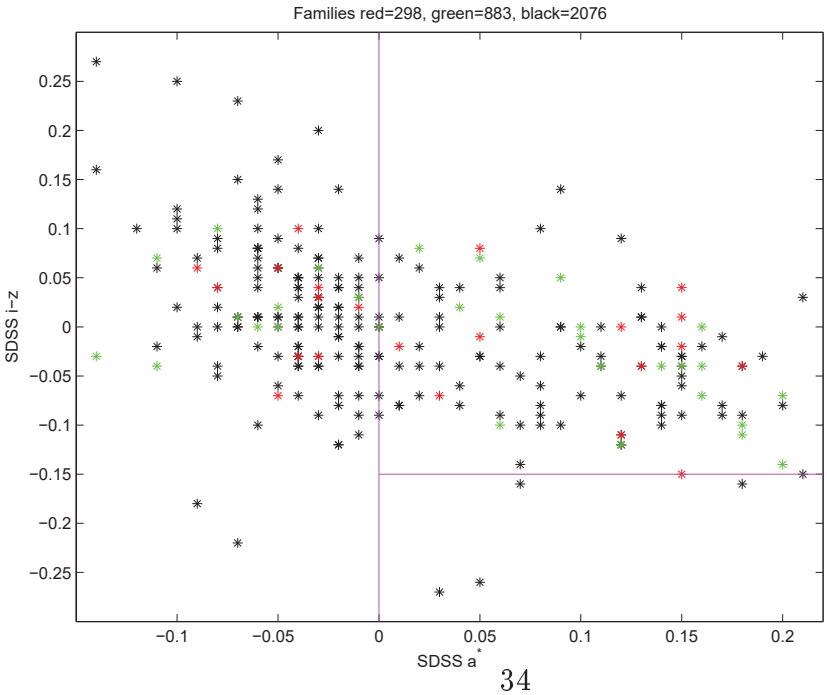

Figure 21: Distribution in the plane of SDSS color indexes a^* and $i-z$ for the members of families 298 (red), 883 (green), 2076 (black). The magenta lines separate the regions mosly occupied by the three taxonomic complexes C (left), S (right above), V (right below).

make the problem more difficult, because all three families appear heterogeneous in composition; the same result is obtained by using WISE albedo data. Therefore we have abstained from merging these three families, in spite of the intersections, and we have computed only one age from the one-sided V-shape of 2076 (Paper III). In the literature there are several "Baptistina families" with rather different membership, conflicting age estimates and conjectures on composition, all based on the assumption that there is just one collisional family.

To solve this problem more physical observations are needed; they should be of high quality and for a large enough set of asteroids in each of the three families.

5.3. The Eos family

The family of (221) Eos is not a problem, in that most of its membership is well known and a single age has been computed (Paper IV). However, interlopers with low albedo could belong to another family formed by cratering of (423) Diotima, which is much larger than (221). Targeted physical observations in the region near (423) in proper elements space are required to confirm the existence of this separate but completely overlapping family.

Another problem is about the family of (179) Klytaemnestra, which is very close in proper elements space to the family 221 but has no intersections with it. This family V-shape in $(a, 1/D)$ has a consistent collisional interpretation neither with 1 nor with 2 collisions. The only explanation we may propose is that family 179 could be contaminated by a large number of interlopers (in the low a portion) transported from family 221, possibly through the secular resonance $g + s - g_6 - s_6$, well known to affect Eos family (Milani and Knežević, 1992; Vokrouhlický et al., 2006). This could be confirmed by physical observations of two sets of asteroids, belonging to 221 and 179, respectively, but close in proper elements space.

5.4. The Adeona family

To be able to compute an age for the family of (145) Adeona, we had to discard a comparatively large number of interlopers, based on the existing physical data. Additionally, there are many outliers for the slope fit for which we have no physical data. A precisely targeted campaign of physical observations of members of the dynamical family 145 with $a < 2.64$ and $5 < D < 15$ km could either confirm our results, including the age, or suggest another interpretation, like the existence of a subfamily.

5.5. The Gersuind family

The family of (686) Gersuind, emerged from the dynamical family 194, may be interesting in connection with the problem of the Barbarians, asteroids with peculiar polarimetric properties (Cellino et al., 2006)). Several Barbarians were found in the neighboring family of (729) Watsonia ((Cellino et al., 2014)). After the removal of the dark and too bright interlopers from 194, the family 686 has albedo properties very similar to 729. Thus the members of 686 should be subjected to investigation with polarimetry.

5.6. The super-Hilda family

The extended Hilda family we discussed in Section 2.1 is only a proposal, for which we do not have a statistically significant confirmation. On the other hand, if it was really there, it would be especially interesting as one of the oldest families. Given the difficulty of getting confirmation from physical observations (essentially all the asteroids in the Hilda region for which data are available are P types, with low albedo), the only way to test the "super-Hilda hypothesis" observationally is to discover more Hildas in the medium inclination region. It should be possible to exclude that the very shallow size distribution is due to observational selection by pushing the complenesss of the catalogs down to $D = 4$ km. Then this would confirm that the alleged super-family is indeed strongly eroded, thus very ancient.

6. Conclusions

In this paper we have attempted to give a collisional model to a number of families for which the same attempt had previously failed. Most of these families were either locked in resonances or anyway significantly affected by resonances, both mean motion and secular. To estimate an age for the family required in each of these resonant cases to apply a specific calibration for the Yarkovsky effect, which in principle could be different in each case.

For the largest families found in the Hilda region, consisting of asteroids locked in the 3/2 resonance with Jupiter, the Yarkovsky effect results in a secular change in eccentricity, thus the V-shape technique had to be applied in the $(e, 1/D)$ plane. There we found family 1911 with a good age determination and family 153 of the *eroded* type, that is which can be seen visually in the plots in the proper $(\sin I, e)$ plane but cannot be confirmed by the statistical tests of the HCM method. If such a family exists, then its age

must be > 3.5 Gy, extremely ancient or even primordial, which is consistent with the hypothesis that this family is depleted to the point of not having a significant density contrast with the background.

For the Trojans, that is the asteroids locked in 1/1 resonance with Jupiter, we are presenting in this paper a new classification which identifies a number of families by using synthetic proper elements and a full HCM method. HCM is well established and has been succesfully applied to the main asteroid belt, but the results in the Trojan swarms indicate that families there have a very different structure. Numerical calibrations have shown that the Yarkovsky perturbations are ineffective in determining secular changes in all proper elements. This implies that all Trojan families are *fossil* families, frozen with the original field of relative velocities, which are small for cratering families, for the fragmentation case somewhat larger, but still limited to the order of the escape velocity from the parent body. Thus we find no way to estimate the ages of the families, while they can be a reliable source of information on the original velocity field immediately after the collision.

We have found a new family among the Griquas, locked in the 2/1 resonance with Jupiter.

We have analysed 6 large families affected by secular resonances, mostly the nonlinear ones. We have used a numerical calibration method, which has shown in all cases that the secular resonances do not affect significanly the secular change of proper a, thus the V-shape method in the $(a, 1/D)$ plane can be used to compute the age in the standard way (as in Paper III).

The solution of some of the cases has been possible only by removal of a number of assumed interlopers. This applies especially to family 145 which otherwise would appear to have a double V-shape.

In conclusion, with the 10 ages computed in this paper, the situation is the following: of the 25 families with > 1000 members, we have computed at least one age for all but 490, which has a too recent age, already known, unsuitable for our method. Of the 19 families with $300 < N < 1000$ members, excluding 778 which has a too recent age, already known, there is only one case left without age, namely 179 (see Section 5.3).

Of the 24 families with $100 < N < 300$ we have computed 6 ages, the others we believe could only give low reliability results. In this range only for families with a small range in proper a we can compute a reliable slope. Thus we can compute only young to medium old ages (< 200 My). As an example, the family of (1222) Tina, with only 137 members, has a short a range and appears to have a well defined V-shape in $(a, 1/D)$, but the

inverse slopes on the two sides are incompatible ($1/S = -0.054 \pm 0.007$ IN, 0.032 ± 0.003 OUT), thus we should conclude it is the result of two separate collisions. With so few data points, this does not appear a mature result, but something to be reanalysed when the number of members is at least doubled.

Among the problems with family ages we have left open, there are three complex families which we believe have more ages than we have estimated: 221, 135, and 298. Two apparently complex cases we believe have been solved: 145, 283, although some confirmation would be useful for 145.

Overall, we believe we have completed a useful work, which is based on the dataset of proper elements we have produced, and by using physical data only as check (apart from absolute magnitudes used for ages). We think it is anyway a good start towards the goal of an absolute chronology of the main collisions in the asteroid main belt, see in Figure 22 all the family ages we have been able to compute so far (in Papers III, IV, and the present one). We have used for the error bars, for the cases where two values IN and OUT are available and compatible, standard deviations computed by the formulae from Milani and Gronchi (2010)[Section 7.2], applicable to all the cases in which two least square fits can be merged under the assumption that the parameters to be determined are the same. This needs to be applied to the term in the error budget due to the fit of the two slopes, under the assumption that they are two solutions for the same physical quantity. Thus the two fits for the slopes reinforce each other (if compatible), while the calibrations are affected by the same errors (e.g., in the density). This more complex formula is an improvement with respect to what we did in Paper III:

$$\sigma_{FIT} = \frac{\sigma_{FITIN}\sigma_{FITOUT}}{\sqrt{\sigma^2_{FITIN} + \sigma^2_{FITOUT}}}$$

$$\sigma_{CAL} = \sqrt{\frac{\sigma^2_{CALIN} + \sigma^2_{CALOUT}}{2}} \qquad \sigma = \sqrt{\sigma^2_{FIT} + \sigma^2_{CAL}}$$

Given our complete open data policy anyone can try by himself to compute other ages with our proper elements and family classification data[9]. However, we recommend caution: ages computed with insufficient data could be unreliable. It is also possible to improve ages (and decrease uncertainty) by using our computed slopes but revising the Yarkovsky calibration with a specific effort for each individual family.

[9]http://hamilton.dm.unipi.it/astdys/index.php?pc=5

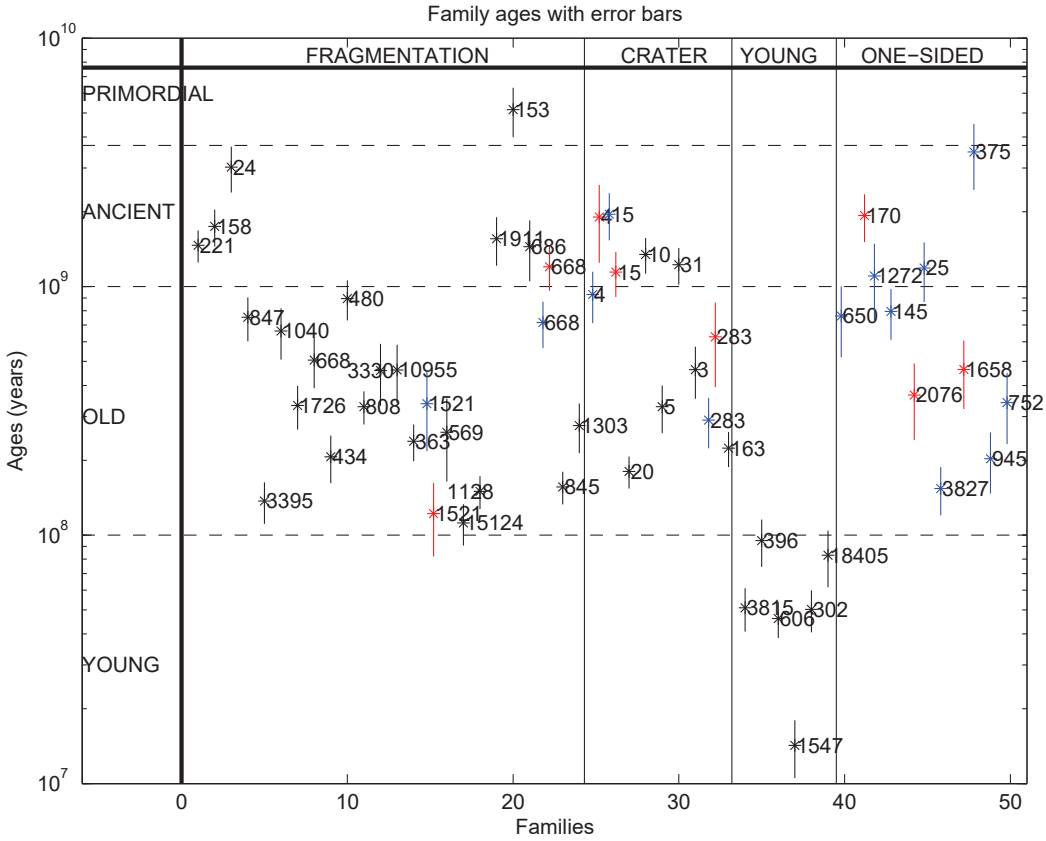

Figure 22: Chronology of the asteroid families; the grouping on the horizontal axis correspond to fragmentation families, cratering families, young families and families with one-sided V-shape (be they cratering or fragmentation).

Acknowledgments

The authors have been supported for this research by: ITN Marie Curie "STARDUST – the Asteroid and Space Debris Network" (FP7-PEOPLE-2012-ITN, Project number 317185) (A.M., Z.K, B.N., and G.T.), the Department of Mathematics of the University of Pisa (A.M.), and the Ministry of Education, Science and Technological Development of Serbia, under the project 176011 (Z.K., B.N.). F.S. is a fellow of the CNES postdoctoral program - project called "Asteroid observations in the Gaia era".

References

References

Bottke, W.F., D. Vokrouhlický, M. Brož, D. Nesvorný, & A. Morbidelli: 2001, Dynamical Spreading of Asteroid Families by the Yarkovsky Effect, *Science* **294** 1693–1696

Bottke W.F., D. Vokrouhlický, D.F. Rubincam & M. Brož: 2002. The effect of Yarkovsky Thermal Forces on the Dynamical Evolution of Asteroids and Meteoroids, in *Asteroids III*, (W.F. Bottke Jr. et al., Eds), University of Arizona Press Tucson, pp. 395–408.

Brož, M., D. Vokrouhlický, A. Morbidelli, D. Nesvorný & W.F. Bottke: 2011, Did the Hilda collisional family form during the late heavy bombardment?, *MNRAS* **414**, 2716–2727.

Cellino, A., V. Zappalà, A. Doressoundiram, M. Di Martino, Ph. Bendjoya, E. Dotto, & F. Migliorini: 2001, The Puzzling Case of the Nysa-Polana Family, *Icarus* **152**, 225–237.

Cellino A., S. J. Bus, A. Doressoundiram, & D. Lazzaro: 2002, Spectroscopic properties of asteroid families, in *Asteroids III*, (W. F. Bottke Jr., A. Cellino, P. Paolicchi, & R. P. Binzel, Eds), University of Arizona Press, Tucson, pp. 633–643.

Cellino A., I.N. Belskaya, Ph. Bendjoya, M. Di Martino, R. Gil-Hutton, K. Muinonen, & E.F. Tedesco: 2006, The strange polarimetric behavior of Asteroid (234) Barbara, *Icarus* **180**, 565–567.

Cellino A., S. Bagnulo, P. Tanga, B. Novaković, & M. Delbò: 2014, A successful search for hidden Barbarians in the Watsonia asteroid family, *MNRAS Letters* **439**, L75–L79.

De León J., N. Pinilla-Alonso, M. Delbo, H. Campins, A. Cabrera-Lavers, P. Tanga, A. Cellino, Ph. Bendjoya, J. Gayon-Markt, J. Licandro, V. Lorenzi, D. Morate, K.J. Walsh, F. DeMeo, Z. Landsman, & V. Ali-Lagoa: 2016, Visible spectroscopy of the Polana-Eulalia family complex: Spectral homogeneity, *Icarus* **266**, 57–75.

Devogele M., A. Cellino, J.P. Rivet, S. Bagnulo, C. Pernechele, D. Vernet, G. Massone, L. Abe, & P. Tanga: 2016, The Calern Asteroid Polarimetric Survey using the Torino Polarimeter: assessment of instrument performances and first scientific results, submitted to *MNRAS*.

Dykhuis M.J. & R. Greenberg: 2015, Collisional family structure within the Nysa-Polana complex, *Icarus* **252**, 199–211.

Grav, T., A. K. Mainzer, J. Bauer, J. Masiero, T. Spahr, R. S. McMillan, R. Walker, R. Cutri, E. Wright, P. R. Eisenhardt, E. Blauvelt, E. DeBaun, D. Elsbury, T. Gautier, S. Gomillion, E. Hand, & A. Wilkins: 2012, WISE/NEOWISE observations of the Hilda population: preliminary results. *Astrophys. J.* **744**, Issue 2, article id. 197, 15 pp.

Knežević Z. & A. Milani: 2000, Synthetic proper elements for outer main belt asteroids. *Cel. Mech. Dyn. Astron.* **78**, 17–46.

Knežević Z. & A. Milani: 2003, Proper element catalogs and asteroid families. *Astron. Astrophys.* **403**, 1165–1173.

Knežević, Z., A. Milani, A. Cellino, B. Novaković, F. Spoto, & P. Paolicchi: 2014. Automated Classification of Asteroids into Families at Work. *Proceedings IAU Symposium 310: Complex Planetary Systems* (Z. Knežević and A. Lemaitre, Eds.) Cambridge Univ. Press., pp 130–133.

Masiero, J.R., A. K. Mainzer, T. Grav, J. M. Bauer, R. M. Cutri, J. Dailey, P. R. M. Eisenhardt, R. S. McMillan, T. B. Spahr, M. F. Skrutskie, D. Tholen, R. G. Walker, E. L. Wright, E. DeBaun, D. Elsbury, T. Gautier IV, S. Gomillion, & A. Wilkins: 2011, Main belt asteroids with WISE/NEOWISE. I. Preliminary albedos and diameters. *Astrophys. J.* **743**, Issue 2, article id. 156, 17 pp.

Migliorini, F., V. Zappalà, R. Vio, & A. Cellino: 1995, Interlopers within Asteroid Families. *Icarus* **118**, 271–291.

Milani A.: 1992, Proper elements for Trojan asteroids, *B.A.A.S.*, **24**, 963.

Milani A.: 1993, The Trojan asteroid belt: Proper elements, stability, chaos and families, *Cel. Mech. Dyn. Astron.*, **57**, 59–94.

Milani, A. & G. F. Gronchi: 2010, *Theory of Orbit Determination*, Cambridge Univ. Press.

Milani, A., & Z. Knežević: 1992, Asteroid proper elements and secular resonances, *Icarus* **98**, 211–232.

Milani, A., & Z. Knežević: 1994, Asteroid proper elements and the Dynamical Structure of the Asteroid Main Belt, *Icarus* **107**, 219–254.

Milani A., A. Cellino, Z. Knežević, B. Novaković, F. Spoto, & P. Paolicchi: 2014, Asteroid families classification: Exploiting very large datasets, *Icarus* **239**, 46–73.

Milani, A., F. Spoto, Z. Knežević, B. Novaković, & G. Tsirvoulis: 2016, Families classification including multiopposition asteroids, *Proceedings IAU Symposium 318: Asteroids: New Observations New Models*,(S. R. Chesley, A. Morbidelli, R. Jedicke & D. Farnocchia, Eds.), Cambridge Univ. Press, pp. 28-45.

Novaković, B., A. Cellino, & Z. Knežević: 2011, Families among high-inclination asteroids, *Icarus* **216**, 69–81.

Paolicchi, P. & Z. Knežević: 2016, Footprints of the YORP effect in asteroid families. *Icarus*, **274**, 314–326.

Radović, V., & Novaković, B.: 2014, Excluding interlopers from asteroid families, *Proceedings IAU Symposium 310: Complex Planetary Systems* (Z. Knežević and A. Lemaitre, Eds.) Cambridge Univ. Press., pp 174–175.

Schubart, J.: 1991, Additional results on orbits of Hilda-type asteroids, *Astron. Astrophys.* **241**, 297–302.

E.A. Smirnov & Shevchenko, I.I.: 2013, Massive identification of asteroids in three-body resonances, *Icarus* **222**, 220–228.

Spoto F., A. Milani, & Z. Knežević: 2015, Asteroid family ages, *Icarus* **257**, 275–289.

Tedesco, E.F., P.V. Noah, M. Noah, & S.D. Price: 2002, The Supplemental IRAS Minor Planet Survey. *Astron. J.* **123**, 1056–1085.

Vinogradova, T.A.: 2015, Identification of asteroid families in Trojans and Hildas, *MNRAS*, **454**, 2436–2440.

Vokrouhlický D., Brož M., Morbidelli A., Bottke W.F., Nesvorný D., Lazzaro D. & A.S. Rivkin: 2006, Yarkovsky footprints in the Eos family, *Icarus* **182**, 92–117.

Walsh K.J., M. Delbo, W.F. Bottke, D. Vokrouhlický, & D.S. Lauretta: 2013, Introducing the Eulalia and new Polana asteroid families: Re-assessing primitive asteroid families in the inner Main Belt, *Icarus* **225**, 283–297.

Zappalà, V., A. Cellino, P. Farinella, & Z. Knežević: 1990, Asteroid families. I - Identification by hierarchical clustering and reliability assessment, *Astron. J.*, **100**, 2030–2046.

Zappalà V., Ph. Bendjoya, A. Cellino, P. Farinella, & C. Froeschlé: 1995, Asteroid families: Search of a 12,487-asteroid sample using two different clustering techniques, *Icarus*, **116**, 291–314.

Appendix: Data for the ages estimation

Table 1: Fit region: family number and name, explanation of the choice, minimum and maximum value of proper e, minimum and maximum value of the diameter selected for the inner and the outer side.

	IN side		OUT side	
Number/name	Min proper e	Min D	Max proper e	Min D
1911 Schubart	0.16	5.00	0.22	6.67
153 Hilda	0.08	10.00	0.29	6.67

Table 2: Fit region: family number and name, explanation of the choice, minimum and maximum value of proper a, minimum and maximum value of the diameter selected for the inner and the outer side.

	IN side			OUT side		
Number/name	Cause	Min a	Min D	Cause	Max a	Min D
110 Lydia	8/3J	2.704	2.50	Ceres	2.767	2.50
194 Prokne	3/1J	2.52	3.33	FB	2.66	3.45
5 Astraea	FB	2.555	2.00	2J+2S-1A	2.61	2.22
283 Emma	9/4J	3.03	6.67	11/5J	3.072	4.00
145 Adeona	FB	2.58	3.33	8/3J	2.7	
25 Phocaea	7/2J	2.26	2.50	YORP?	2.45	
945 Barcelona	FB	2.59	1.25	11/4J	2.65	

Table 3: Family albedos: number and name of the family, albedo of the largest body with its standard deviation and code for source (W=WISE, I=IRAS), maximum and minimum albedo values for computing mean, mean and standard deviation of the albedo of the members with $S/N > 3$ WISE data. For the Hilda region we have used the values of the mean albedo and STD from Grav et al. (2012).

	Largest Body			Family Albedo			
Number/name	Albedo	STD	Ref.	Min	Max	Mean	STD
110 Lydia	0.170	0.042	W		0.15	0.073	0.020
1911 Schubart	0.025	0.001	I			0.039	0.013
153 Hilda	0.062	0.002	I			0.061	0.011
194 Prokne	0.142	0.004	W	0.08	0.25	0.145	0.040
5 Astraea	0.245	0.051	W	0.10	0.50	0.269	0.076
283 Emma	0.032	0.004	W		0.10	0.049	0.013
145 Adeona	0.043	0.013	W		0.10	0.062	0.010
25 Phocaea	0.231	0.024	I		0.60	0.253	0.117
945 Barcelona	0.242	0.024	I		0.50	0.300	0.100

Table 4: Slopes of the V-shape for the families in the 3/2 resonance: family number/name, side, slope (S) in the $(e, 1/D)$ plane, inverse slope ($1/S$), standard deviation of the inverse slope, ratio OUT/IN of $1/S$, and standard deviation of the ratio.

Number/name	Side	S	$1/S$	STD $1/S$	Ratio	STD ratio
1911 Schubart	IN	-3.845	-0.260	0.028		
	OUT	3.703	0.270	0.020	1.04	0.13
153 Hilda	IN	-1.038	-0.963	0.084		
	OUT	0.998	1.002	0.147	1.04	0.18

Table 5: Slopes of the V-shape for the families: family number/name, side, slope (S) in the $(a, 1/D)$ plane, inverse slope ($1/S$), standard deviation of the inverse slope, ratio OUT/IN of $1/S$, and standard deviation of the ratio. Note the change of the family namesakes, 110 to 363, 194 to 686.

Number/name	Side	S	$1/S$	STD $1/S$	Ratio	STD ratio
363 Padua	IN	-5.972	-0.168	0.027		
	OUT	7.844	0.128	0.112	0.76	0.14
686 Gersuind	IN	-1.758	-0.569	0.322		
	OUT	1.874	0.534	0.138	0.94	0.58
5 Astraea	IN	-7.942	-0.126	0.029		
	OUT	8.467	0.118	0.028	0.94	0.31
283 Emma	IN	-6.046	-0.165	0.019		
	OUT	2.814	0.355	0.112	2.15	0.72
145 Adeona	IN	-2.014	-0.497	0.058		
25 Phocaea	IN	-2.122	-0.471	0.047		
945 Barcelona	IN	-13.445	-0.074	0.014		

Table 6: Data for the Yarkovsky calibration: family number and name, proper semimajor axis a and eccentricity e for the inner and the outer side, $1 - A$, density value ρ at $D = 1$ km, taxonomic type, a flag with values m (measured) a (assumed) g (guessed), and the relative standard deviation of the calibration.

	IN side		OUT side		Tax				
Numb/name	a	e	a	e	1-A	ρ	typ	Fl	STD
363 Padua	2.70	0.04	2.78	0.04	0.97	1.41	C	m	0.20
1911 Schubart	3.963	0.145	3.967	0.214	0.98	1.41	P	g	0.30
153 Hilda	3.95	0.07	4.00	0.30	0.98	1.41	P	g	0.30
686 Gersuind	2.52	0.175	2.66	0.175	0.95	2.275	S	m	0.20
5 Astraea	2.56	0.18	2.60	0.19	0.93	2.275	S	m	0.20
283 Emma	3.03	0.115	3.07	0.115	0.98	1.41	C	m	0.20
145 Adeona	2.58	0.162			0.98	1.41	C	m	0.20
25 Phocaea	2.26	0.215			0.92	2.275	S	a	0.25
945 Barcelona	2.60	0.24			0.90	2.275	S	m	0.20

Table 7: Age estimation for the families in the 3/2 resonance: family number and name, calibration de/dt, age estimation, uncertainty of the age due to the fit, uncertainty of the age due to the calibration, and total uncertainty of the age estimation.

Numb/name	Side	de/dt	Age	STD_{FIT}	STD_{CAL}	STD_{AGE}
		$10^{-4}/My$	My	My	My	My
1911 Schubart	IN	-1.68	1547	165	464	492
	OUT	1.72	1566	115	470	484
153 Hilda	IN	-1.83	5265	461	1580	1645
	OUT	1.99	5039	737	1512	1682

Table 8: Age estimation for the families: family number and name, calibration da/dt, age estimation, uncertainty of the age due to the fit, uncertainty of the age due to the calibration, and total uncertainty of the age estimation.

Numb/name	Side	da/dt $10^{-4}au/My$	Age My	STD_{FIT} My	STD_{CAL} My	STD_{AGE} My
363 Padua	IN	-5.90	284	46	57	73
	OUT	5.82	219	19	44	48
686 Gersuind	IN	-3.82	1490	843	298	894
	OUT	3.62	1436	371	287	469
5 Astraea	IN	-3.72	339	79	68	104
	OUT	3.70	319	74	64	98
283 Emma	IN	-5.69	290	33	58	67
	OUT	5.66	628	197	126	234
145 Adeona	IN	-6.25	794	92	159	184
25 Phocaea	IN	-3.97	1187	117	297	319
945 Barcelona	IN	-3.66	203	38	41	56